

Renewable electricity capacity planning with uncertainty at multiple scales

Michael C. Ferris¹ and Andy Philpott²

¹Computer Sciences Department and Wisconsin Institute for Discovery, University of Wisconsin-Madison, Madison, WI, 53706.

²Electric Power Optimization Centre, University of Auckland, Auckland, New Zealand.

Contributing authors: ferris@cs.wisc.edu;
a.philpott@auckland.ac.nz;

Abstract

We formulate and compare optimization models of investment in renewable generation using a suite of social planning models that compute optimal generation capacity investments for a hydro-dominated electricity system where inflow uncertainty results in a risk of energy shortage. The models optimize the **expected** cost of capacity expansion and operation allowing for investments in hydro, geothermal, solar, wind, and thermal plant, as well as battery storage for smoothing load profiles. A novel feature is the integration of uncertain seasonal hydroelectric energy supply and short-term variability in renewable supply in a two-stage stochastic programming framework. The models are applied to data from the New Zealand electricity system and used to estimate the costs of moving to a 100 % renewable electricity system by 2035. We also explore the outcomes obtained when applying different forms of CO₂ constraint that limit respectively non-renewable capacity, non-renewable generation, and CO₂ emissions on average, almost surely, or in a chance-constrained setting, and show how our models can be used to investigate the merits of a proposed pumped-hydro scheme in New Zealand's South Island.

Keywords: renewable electricity, carbon price, climate change

1 Introduction

In this paper we study investment in renewable generation under uncertainty. There has been much attention devoted to capacity planning models to design electricity systems that will deliver (close to) 100 % renewable electricity. In most electricity systems renewable energy comes from either wind power or solar energy. Since this is intermittent, the planning problem must account for uncertainty. Renewable energy can also come from hydroelectricity and geothermal power. Inflows to hydroelectricity reservoirs are uncertain, but at a different time-scale, and in many cases there is some control over their release. Run-of-river hydroelectric plants on the other hand convert uncertain inflows into uncertain levels of energy. Geothermal power is more predictable (although exploration involves significant uncertainties at the design stage), but after drilling it is a reliable base-load energy source. Finally nuclear power is typically treated as non-renewable, but can be a useful technology if greenhouse gas emissions are to be reduced. Failure scenarios are very infrequent but extremely costly.

When the generation of electricity comes from sources with uncertain fuel supply, some care must be taken in defining 100 % renewable. The strictest definition would admit no non-renewable generation under any realization of the uncertainty. One would expect this to be very expensive in terms of both capital investment and operating cost. In New Zealand, the Government is seeking an electricity system that is 100 % renewable in a normal hydrology year. This could be interpreted in a number of ways. One option is to model this as a chance constraint: *i.e.*, the probability of any year having 100 % renewable generation is at least $1 - \alpha$, where α is chosen appropriately. We show in our calculations that such a policy is not guaranteed to have low emissions when averaged over all possible hydrological years, while being more expensive than competing plans in terms of capital and operating costs.

In this paper we develop a suite of models for investment in renewable generation that incorporate 100 % renewable constraints in a variety of ways. We study two forms of storage that might make such a constraint easier to satisfy. Within a day, battery storage can be used to transfer energy between time periods. This can be used to accommodate more intermittent energy (wind and solar) that otherwise would be wasted. Over a longer time horizon, hydroelectric reservoir storage can be used to transfer energy from season to season to account for low seasonal inflows. We provide mathematical models for both these phenomena, and demonstrate their usefulness on an example based on New Zealand data.

The contributions of our paper are as follows.

1. We describe how to incorporate multiple scales of uncertainty into a two-stage electricity planning model.
2. We expose the effects of **adopting different performance indicators on the outcomes of the models.**

3. We show how imposing plausible constraints on non-renewable capacity (e.g. as a political position) might lead to suboptimal outcomes.

One concern is for markets with a lot of stored hydroelectricity (such as New Zealand) that provide plenty of ramping capacity. We provide examples of the use of our model for supply adequacy when reservoir inflows, wind, and solar energy are uncertain or variable. To do this we shall use New Zealand as a case study and build up a new screening curve stochastic optimization model for capacity planning that accommodates this. We create the first stochastic system optimization model of the New Zealand electricity system, explicitly targeted to CO₂ emission reduction, and focusing on the interrelationship between uncertain seasonal hydroelectricity energy supply and short term changes in wind and solar supply. We illuminate the differences between applying different forms of CO₂ constraint. Imposing regulatory constraints (such as dictating 100 % renewable capacity) without careful thought can lead to unforeseen outcomes. Our model shows that one should focus on constraining CO₂ emissions: the outcomes from solving the model then give the mix of generation plant that one might hope to see. In particular we investigate constraints on non-renewable capacity, non-renewable generation, CO₂ emissions, and a chance constraint that limits the frequency of years that use non-renewable generation.

Our focus in this paper is on a central planning model for optimizing the mix of generation plant to reach New Zealand's net-zero carbon objectives expressed in various forms. The results of this model give a first-best solution that one might aim for by choosing appropriate policy settings. New Zealand has an energy-only wholesale electricity pool market in which generation investments are made on a commercial basis. It also has an emissions trading scheme that requires CO₂-emitting entities to surrender CO₂ permits that are bought and sold by auction on a regular basis. The price of these permits responds to emissions budgets that are recommended by the New Zealand Climate Change Commission. The models in this paper give some indication of the minimum extra costs faced by the electricity system of setting these budgets.

The social planner in our models is assumed to be risk neutral. Commercial investors in electricity generation capacity are typically risk-averse, and so are sensitive to the volatility of electricity prices and emission prices. We have chosen in this paper to ignore these aspects which we continue to explore in related work [Ferris and Philpott \(2023\)](#). A full study of price volatility and its effect on investment requires a risked competitive equilibrium model where risk-averse investors choose capacities and operations to maximize risk-adjusted expected returns at equilibrium prices. In the absence of a complete market for risk, this equilibrium will in general not have the same outcomes as a risk-averse central planning model and the prices that emerge from this model as dual variables (see, e.g., [Ralph and Smeers \(2015\)](#) and [Kok et al \(2018\)](#)).

The paper is laid out as follows. In the next section we describe deterministic and stochastic social planning models for investment in electricity systems with stored hydro. In section 3 we describe three approaches to model the reduction in CO₂ emissions. Section 4 describes the calibration of our model to the New Zealand electricity system, and section 5 presents some selected results from applying this calibrated optimization model to investigate some specific questions arising from the New Zealand Government policy of a 100 % renewable electricity system by 2035. Section 6 concludes the paper with a discussion of results.

2 Social planning model for investment

2.1 Conventional capacity expansion models

Classical electricity capacity planning models [Stoft \(2002\)](#); [Joskow \(2006\)](#) use a *screening curve* to rank generation options by their long-run marginal cost (LRMC), thus finding the best option to serve the production profile for each additional demand unit. The screening curve shows the annual total cost per MW capacity plotted against the number of annual operating hours. The total cost is a combination of fixed and variable cost based on the number of production hours in a year. A minimum cost for each capacity factor can be found by combining the screening curve with the *load duration curve* (LDC). To supply the part of the LDC that has higher capacity factor (*i.e.*, running most of the year), base load is the least cost option. As the number of operating hours decreases, the plants that are less expensive to build but more costly to run begin to become more economical. For a small number of hours at the tip of the duration curve, high variable cost peakers are the most economical. Finally, there is a small piece of peak load that will not be met. When this happens electricity price will take the value of lost load (VOLL) if demand is inelastic or the marginal value of load in the elastic demand case. In a market setting, the difference between these prices and the short-run marginal cost of peaking generation provides the necessary rent to cover the fixed cost of the peaking plant (as well as contributing to cover fixed cost on all the other plants).

In simple cases, the screening curve solution can be found by inspection. When the LDC is piecewise constant, it is the solution to the linear program

$$\begin{aligned}
 \text{LP: min} \quad & \psi = \sum_{k \in \mathcal{K}} (K_k x_k + L_k z_k) + Z \\
 \text{s.t.} \quad & Z = \sum_{b \in \mathcal{B}} H_b \left(\sum_{k \in \mathcal{K}} C_k y_{k,b} - V(d_b - r_b) \right), \\
 & 0 \leq x_k \leq X_k, \quad k \in \mathcal{K}, \\
 & 0 \leq z_k \leq x_k + U_k, \quad k \in \mathcal{K}, \\
 & 0 \leq y_{k,b} \leq z_k, \quad k \in \mathcal{K}, b \in \mathcal{B}, \\
 & 0 \leq r_b \leq d_b, \quad b \in \mathcal{B}, \\
 & d_b \leq \sum_{k \in \mathcal{K}} y_{k,b} + r_b, \quad b \in \mathcal{B}.
 \end{aligned}$$

where

- $k \in \mathcal{K}$ denotes different generating technologies;
- $b \in \mathcal{B}$ indexes load blocks where H_b denotes the number of hours in block b , and $\sum_{b \in \mathcal{B}} H_b$ gives the number of hours in a year;
- U_k is existing capacity (MW) of technology k ;
- the variable x_k is additional capacity (MW) in technology k , constrained by upper bound X_k ;
- the variable z_k is the new capacity (MW) after investing in technology k ;
- variable cost for technology k is defined as C_k (\$/MWh) respectively;
- annual capital cost for technology k is defined as K_k (\$/MWh p.a.);
- annual maintenance cost for technology k is defined as L_k (\$/MWh p.a.);
- the load in load block b is d_b , and value of lost load is V (\$/MWh);
- $y_{k,b}$ denotes the production (MW) of technology k in each hour in load block b ;
- r_b denotes the load shed (MW) in each hour in load block b .

2.2 Relation to previous work

Formulations like LP appeared as early as the 1950s [Masse and Gibrat \(1957\)](#), although the basic formulation has been extended in the past two decades to include operational constraints, and some supply-side uncertainties such as plant outages and technological changes were added. Demand distributions are still represented by load duration curves, or their discretized versions [De Jonghe et al \(2012\)](#). A number of authors (see, *e.g.*, [Bishop and Bull \(2008\)](#)) have extended LP to include binary capital planning decisions (so z_k takes on discrete values) and planning over multiple years to accommodate growing demand.

Not surprisingly, models for studying the decarbonization of energy systems are receiving considerable attention in the literature. Many of these models, for example [Graf and Marcantonini \(2017\)](#), focus on the intermittency of renewables and the effect of this on backup thermal generation and/or storage. The investment paths of these models are either prescribed in advance or simulated by estimating net present values of candidate investments at each stage and then incrementing the model by one time step with selected investments in place.

Our model is closer in spirit to the classical system planning models such as MARKAL [Fishbone and Abilock \(1981\)](#) and its modern implementation in the TIMES system [Loulou and Labriet \(2008\)](#); [Loulou \(2008\)](#). Other similar planning models are ReEDS [Short et al \(2011\)](#) and GEM [Bishop and Bull \(2008\)](#). Our model extends these to include uncertainty in operations. In its simplest form, this gives a two-stage model in which stage one invests in capacity and stage 2 operates this in different states of the world. A multistage version would invest in capacity over several stages, and in each stage operate the system subject to the realized uncertainty in operating conditions.

A number of authors have developed models similar to ours. In the United States, [Boffino et al \(2019\)](#) study the effect of emissions reduction in ERCOT, the Texas electricity market. Their model includes wind variation, but Texas

has no hydro reservoirs, so the ERCOT model does not model uncertainty in energy supply, a criterion that is critical for New Zealand. Similar models to that in [Boffino et al \(2019\)](#) have emerged for Europe, for example the EMPIRE model for capacity expansion developed by [Skar et al \(2014\)](#). Similar to our model, EMPIRE restricts capacities of generators using a stochastic availability factor (for *e.g.* wind and run-of-river plant), but their treatment of hydro storage is more simple than ours, constraining total reservoir hydro generation for each reservoir by a seasonal energy constraint. In recent work [Domínguez et al \(2021\)](#) examine capacity expansion in Europe using a multistage stochastic programming model with stochastic dominance constraints on carbon emissions relative to European Commission benchmarks.

In the following sections we describe our model as it is applied to the New Zealand electricity system. To our knowledge there are no stochastic optimization models of the decarbonization of the New Zealand system. [Mason et al \(2010, 2013\)](#) examine New Zealand historical generation, and estimate levels of renewable generation capacity needed to replace historical thermal generation. Their results are calibrated to historical outcomes in the years 2005-2010. Although the study included a very dry year (2008) any future year with a different (and unknown) hydro inflow sequence and different demand levels might require more renewable capacity than indicated in [Mason et al \(2013\)](#). Our model explicitly includes future demand forecasts and stochastic variation in inflows and wind.

2.3 Stochastic planning model data

In this paper we explore the extent to which uncertainty affects the screening-curve approach. With uncertain supply from renewable energy, the problem LP no longer correctly represents the optimal capital planning problem which now becomes a stochastic linear program. The uncertainty will manifest itself in various ways that we will endeavour to model in a two-stage stochastic modeling framework.

Most stochastic capacity expansion models in the literature are designed to model intermittent wind and solar generation, and determine investments (including peaking generation capacity and batteries) to deal with this. The most common approach to modeling these types of generation is to select several “representative days” from a year to give daily generation scenarios. See [Merrick \(2016\)](#) and references cited therein for a discussion of this approach. [Pineda and Morales \(2018\)](#) show how representative time periods longer than a day can be hierarchically clustered to accommodate inter-day variability.

We have chosen not to use this approach in our models. The inflow variation in our scenarios occurs over weeks or months. Representing intra-day variation too faithfully risks biasing the optimization towards a clairvoyant solution over a longer time scale. Thus we use a model based on load blocks, but extend this to account for uncertainty at shorter time scales. To deal with intra-day storage (*e.g.* from batteries) requires some degree of approximation of operations at the hourly level. For example we ignore investments to deal with ramping

constraints as studied in Wu et al (2017) or Khazaei and Powell (2017). These approximations could potentially be improved by the clever integration of a representative-days model.

Our approach to modeling uncertainty closely follows that of Kok et al (2018) and will motivate the different scales using data collected in 2017 for the New Zealand wholesale electricity market. Since the types of uncertainty we consider have different effects at distinct time-scales, we need two sets of parameters to deal separately with the short-term uncertainty in wind and run-of-river generation, and the medium-term uncertainty in reservoir storage. We do this by introducing a scenario index $\omega \in \Omega$ that represents a random future state of the world. In general, each state of the world ω is a vector of random outcomes. In our model this vector is two dimensional where the first component ω_1 corresponds to a certain type of year, and the second component ω_2 relates to parameter variation in each season t of a year. The effect of these outcomes on the model is represented for each region i by the set of random parameters $\mu_{k,i,b,t}(\omega), \nu_{k,i,t}(\omega), k \in \mathcal{K}, b \in \mathcal{B}$.

The parameter $\mu_{k,i,b,t}(\omega)$ for technology k in region i and season t denotes a proportional reduction in its capacity in load block b and random event ω . Here μ is used in constraints on the generation (recourse variables) $y_{k,i,b,t}(\omega)$ that hold in each of the scenarios ω :

$$y_{k,i,b,t}(\omega) \leq \mu_{k,i,b,t}(\omega) z_{k,i}.$$

Note that $z_{k,i}$ is now indexed by both region i and technology k . Some examples will help illustrate the model.

If $k = 1$ is run-of-river hydroelectricity generation then $\mu_{k,i,b,t}(\omega_1, \omega_2) = \mu_{1,i,b,t}(\omega_1)$, a parameter that depends only on the type of year being experienced that scales down the nominal capacity of the generators in region i to reflect the inflows that occur in season t of that year. For run-of-river plant with intra-day flexibility, the capacity factor $\mu_{1,i,b,t}(\omega_1)$ can depend on the load block, being greater than average in peak times and less in offpeak times, while averaging out to the value corresponding to the season and type of year. We represent this by scaling a base value $\hat{\mu}$ for the plant by a block dependent parameter α , so $\mu_{1,i,b,t}(\omega_1) = \hat{\mu}_{i,t}(\omega_1) \alpha_{i,b,t}$. Values of α can be estimated from historical dispatch records.

If $k = 2$ is wind power, then we might assume that the distribution of wind in a given load block does not depend on that block. (Of course in some cases this will not be true, for example a sea breeze might occur in coastal town in periods close to the evening system peak.). The simplest model assumes that the wind contributes uniformly to the hours in a load block in a region i and season t with a constant load factor $\mu_{2,i,t}(\omega_1)$ that might have several realizations estimated from historical wind generation in each load block. For small amounts of wind this approach is sufficient, but as wind capacity grows, the model becomes less realistic. Historical wind generation data contain many periods with no wind at all, so assuming an average load factor will give a smoother picture than reality, especially in peak periods when a sudden

lack of wind requires peaking plant to be dispatched. We approximate this by including scenarios ω_2 with $\mu_{2,i,b,t}(\omega_1, \omega_2) = 0$ for the peak load block ($b = 1$), having probabilities $p_t(\omega_2)$ estimated from the frequency of historical no-wind hours in the load block. Observe that p_t depends on t , which allows it to vary with season.

If $k = 3$ is solar power then we might assume for example that the insolation depends only on the time of day. (Of course in some cases it will depend on random weather.) Then $\mu_{3,i,b,t}(\omega) = \mu_{3,i,b,t}$ depends only on the load block, region and season. For a technology like stored hydro, say $k = 4$, $\mu_{4,i,b,t}(\omega) = 1$, unless ω_2 corresponds to an outage event with probability α_k , when $\mu_{4,i,b,t}(\omega_1, \omega_2) = 1 - \alpha_k$, the probability that the station is at full capacity.

The parameter $\nu_{k,i,t}(\omega)$ for technology k denotes a proportional reduction in its total annual energy production in region i in season t in a year of type ω . If, as before, $k = 4$ is generation from stored hydroelectric power then the event ω could correspond to lower than average reservoir inflows over a year. In this dry-year event we can still run the reservoir hydro-station turbines at 100 % of their capacity, but not for the whole year. In New Zealand, $\nu_{k,i,t}(\omega)$ for stored hydro is between 0.4 and 0.6, which is the range of capacity factors for hydro stations. If $k = 5$ is thermal plant then $\nu_{5,i,t}(\omega)$ can model random fuel stockpile levels, but typically we assume $\nu_{5,i,t}(\omega) = 1$. Some values of $\mu(\omega)$ and $\nu(\omega)$ estimated from New Zealand historical data are given in Appendix B below, and are also available for download from <https://www.cs.wisc.edu/~ferris/data/100percent>

2.4 Hydroelectric storage

We now complete the model by including storage and transmission variables. Electricity systems with stored hydroelectricity transfer energy from seasons with high inflows (*e.g.*, from snow melt) to seasons with low inflows. In New Zealand this generally corresponds to a transfer of energy from a wet summer to a potentially dry winter. This transfer is profitable not only because winter supply of energy is smaller than summer, but energy demand in winter tends to be higher than in summer.

The most realistic models for optimizing this transfer of energy use stochastic dynamic programming to optimize reservoir releases when inflows are uncertain. For our investment model, such a detailed operational optimization would be too computationally expensive to include, so we must approximate an optimal reservoir release policy. Our approximation adds a time index $t = 0, 1, 2, \dots, T - 1$ to the model, where typically t will denote a season of the year (so $T = 4$). We let s_t denote the water transferred from the end of time interval t to the beginning of time interval $(t + 1) \bmod T$, where we interpret $t = -1$ as the period $T - 1$ of the previous year. Each time interval t can be broken up into load blocks $b \in \mathcal{B}_t$, each having H_b hours. The total number of hours in each time interval is then $\sum_{b \in \mathcal{B}_t} H_b$.

The hydroelectric storage equations use $\nu_{k,i,t}(\omega) \sum_{b \in \mathcal{B}_t} H_b z_{ki}$ which is a measure of the total energy available for hydro generation in time interval t

in scenario ω . Here $\nu_{k,i,t}(\omega)$ can be estimated from the total possible energy $W_t(\omega)$ that could be produced from stored hydro in time interval t in scenario ω . Given a historical year ω we let

$$W_t(\omega) = \text{historical hydro generation in } (t, \omega) + \text{energy stored at the end of } t \\ - \text{energy stored at the start of } t,$$

and set

$$\nu_{k,i,t}(\omega) = \frac{W_t(\omega)}{\sum_{b \in \mathcal{B}_t} H_b z_{k,i}}.$$

In this case, the generation variables are now indexed additionally by t , and the controlling constraint on hydroelectric storage s_t has the following form:

$$\sum_{b \in \mathcal{B}_t} H_b y_{k,i,b,t}(\omega) \leq \nu_{k,i,t}(\omega) \sum_{b \in \mathcal{B}_t} H_b z_{k,i} - s_{i,t} + s_{i,t-1}, \quad (1)$$

along with other physical constraints modeled using $s \in \mathcal{H}$. Typically \mathcal{H} represents simple capacity constraints on the storage in each reservoir, but it could also model limits imposed by environmental constraints (such as minimum levels). Observe that (1) does not define $s_{i,t}$ uniquely and for any i we may add or subtract a constant from $s_{i,t}$ for all t and remain feasible (as long as s remains in \mathcal{H}).

Observe that $\nu_{k,i,t}(\omega)$ can take values larger than 1, if season t in scenario ω corresponds to high inflows, a large part of which are retained as reservoir storage at the end of season t . The energy constraint (1) is accompanied by a generation capacity constraint

$$y_{k,i,b,t}(\omega) \leq \mu_{k,i,b,t}(\omega) z_{k,i},$$

where $\mu_{k,i,b,t}(\omega) = 1$, so (1) may not be binding if there are very large inflows and $s_{i,t}$ is at its capacity (meaning some inflows will be spilt).

In our model, reservoir storage decisions $s_{i,t}$ are chosen in a first stage (for the end of each season) to make (1) feasible for all ω . The operating policy will then be required to drive the storage through these points. This could be overly restrictive, for example, if we had large inflows in season t , in year ω , when it makes sense to choose $s_{i,t-1}$ to be lower just for this year. On the other hand allowing $s_{i,t-1}$ to freely anticipate future inflows removes the need for the variable entirely. We compromise by allowing $s_{i,t}$ to vary around a set point $\bar{s}_{i,t}$ by a limited amount \hat{s} . Thus (1) becomes

$$\sum_{b \in \mathcal{B}_t} H_b y_{k,i,b,t}(\omega) \leq \nu_{k,i,t}(\omega) \sum_{b \in \mathcal{B}_t} H_b z_{k,i} - s_{i,t}(\omega) + s_{i,t-1}(\omega),$$

and

$$s_{i,t}(\omega) \leq \bar{s}_{i,t} + \hat{s},$$

$$s_{i,t}(\omega) \geq \bar{s}_{i,t} - \hat{s}.$$

Here $\bar{s}_{i,t}$ are variables optimized by the model, whereas \hat{s} is an exogenous parameter chosen by the user.

2.5 Battery storage

In contrast to seasonal storage, battery storage in our context represents all devices that can be used to transfer energy between load blocks within a season. This could encompass *e.g.*, conventional electrical batteries, hydrogen production and storage, compressed air storage and hydro pumped storage. These technologies shift load out of peak periods to off-peak periods to reduce the need for peaking plant or extra transmission capacity. Our experiments reported in this paper focus on conventional electrical batteries to perform this task. There are currently no pumped storage facilities in New Zealand.¹

Optimizing battery storage has received a lot of attention in the literature. The paper by Sioshansi *et al.* [Sioshansi et al \(2009\)](#) gives a good overview of the potential benefits of batteries. To determine optimal operating policies for batteries one should ideally solve an infinite horizon stochastic dynamic program [Xi et al \(2014\)](#). With many storage devices (each of which requires a state variable) this becomes too expensive to include within a capacity expansion model. Wu *et al.* [Wu et al \(2017\)](#) explores the limits of this approach using a Markov decision process defined on a reduced state space. Other approaches (that are focused mainly on short-term operations) approximate the optimization of operational decisions using *e.g.*, approximate dynamic programming [Cheng and Powell \(2016\)](#), parameterized decision rules [Egging et al \(2016\)](#), or heuristics based on opportunity cost estimates [Graf and Wozabal \(2013\)](#). Our focus in this paper is to develop a model that can explore the effects of investment in battery storage on seasonal security of energy supply. To do this we require an approximate battery model that provides some realism, but is simple enough that it does not yield an intractable investment model. The model is as follows.

Battery storage is denoted by indices $k \in \mathcal{S} \subseteq \mathcal{K}$, where installed energy capacity in region i is denoted z_{ik} (MWh), and charging in region i and season t is effected by power variables $g_{k,i,b,b',t}(\omega)$ where $b' \neq b$ denotes a load block in which the power charged in b will be discharged. Note that both b and b' are blocks in \mathcal{B}_t , where t is the time period (season). The term

$$\sum_{b' \neq b} g_{k,i,b,b',t}(\omega)$$

is the extra power needed in load block b that will charge the battery k for later discharge. Different battery types with the same storage capacity have different maximum charging rates (and costs). Given battery type $k \in \mathcal{S}_1$, denote by β_k

¹The New Zealand Government is currently investigating constructing such a facility in the South Island, intended primarily for seasonal storage (see section 5.5).

the maximum rate of charge per MWh of storage capacity. Thus installing twice as many batteries doubles the charging rate. This gives a charging constraint

$$\sum_{b' \neq b} g_{k,i,b,b',t}(\omega) \leq \beta_k z_{k,i}, \quad b \in \mathcal{B}_t, k \in \mathcal{S}_1,$$

where $z_{k,i}$ (MWh) is the storage capacity choice for battery type k in region i , and t is the time period (season).

Let the number of days in each time period t be denoted D_t . We assume that each day in a season has the same number of hours in each load block, and the battery operates in the same way on each day. Then $\frac{H_b}{D_t}$ is the number of hours in load block b in any given day in time period t . This means that that total amount that the battery is charged in any block $b \in \mathcal{B}_t$ during a day cycle is

$$\frac{H_b}{D_t} \sum_{b' \neq b} g_{k,i,b,b',t}(\omega).$$

In the worst case, the battery will need to be charged in contiguous hours (*e.g.* overnight) to be discharged in later peak hours. This assumption means that the total amount that a battery will be charged in a day will involve adding the charge over all blocks b where $\sum_{b' \neq b} g_{k,i,b,b',t}(\omega) > 0$. The battery energy capacity z_{ik} (MWh) then restricts the choice of g , with the constraint

$$\sum_b \frac{H_b}{D_t} \sum_{b' \neq b} g_{k,i,b,b',t}(\omega) \leq z_{k,i}, \quad k \in \mathcal{S}.$$

The amount of energy stored in the battery for discharge in block b on a given day will be $\sum_{b' \neq b} \frac{H_{b'}}{D_t} g_{k,i,b',b,t}(\omega)$. Upon discharge this will yield the energy

$$\eta_k \sum_{b' \neq b} \frac{H_{b'}}{D_t} g_{k,i,b',b,t}(\omega)$$

where η_k is the round trip efficiency of the battery. This energy will be spread over the hours in block b on the given day. The power contribution (MW) in each of these hours is then

$$\frac{\eta_k \sum_{b' \neq b} \frac{H_{b'}}{D_t} g_{k,i,b',b,t}(\omega)}{\left(\frac{H_b}{D_t}\right)}$$

which simplifies to

$$\eta_k \sum_{b' \neq b} \frac{H_{b'}}{H_b} g_{k,i,b',b,t}(\omega).$$

2.6 Transmission constraints

The final part of the model defines constraints on the electricity transmission. Transmission from region i to region j in load block b is denoted by $f_{i,j,b,t}(\omega)$, and the net flow arriving at region i from other regions is

$$\sum_j \left(\left(1 - \frac{\alpha_{j,i}}{2}\right) f_{j,i,b,t}(\omega) - \left(1 + \frac{\alpha_{i,j}}{2}\right) f_{i,j,b,t}(\omega) \right) \quad (2)$$

where $\alpha_{i,j}$ is the proportional loss in energy incurred by transmission in the line between i and j . The transmission flows can be restricted by additional constraints $f \in \mathcal{F}$ that model Kirchhoff's voltage constraints from DC-load flow, for example. [In the experiments described below we assume a radial transmission network, so \$\mathcal{F}\$ only imposes capacity constraints on inter-regional flows.](#)

The formula (2) gives a total net supply of power in load block b at region i defined by

$$\begin{aligned} q_{i,b,t}(\omega) = & \sum_{k \in \mathcal{K}_i} y_{k,i,b,t}(\omega) \\ & + \sum_j \left(\left(1 - \frac{\alpha_{j,i}}{2}\right) f_{j,i,b,t}(\omega) - \left(1 + \frac{\alpha_{i,j}}{2}\right) f_{i,j,b,t}(\omega) \right) \\ & - \sum_{k \in \mathcal{K}_i} \sum_{b' \neq b} g_{k,i,b,b',t}(\omega) \\ & + \sum_{k \in \mathcal{K}_i} \eta_k \sum_{b' \neq b} \frac{g_{k,i,b',b,t}(\omega) H_{b'}}{H_b}, \end{aligned}$$

where $\mathcal{K}_i \subseteq \mathcal{K}$ are the technologies available at region i . This constraint assumes that all destination blocks b' occur in the same day as b . This won't necessarily be the case. Some load blocks (representing annual system peaks) have only a few hours in them. One could restrict b' to load blocks that are not too far from b , so shifted load can be assumed to come from the same block. Note that other data such as K_k , L_k , C_k , μ_k , ν_k and D_t can be extended to be location dependent in a straightforward way.

2.7 Demand response

One mechanism for reducing load in peak times is to shift load. With appropriate incentives, consumers can be assumed to not purchase electricity in a peak period for a given activity by deferring it to a period with lower total demand. Typically these shifts of demand are within a day, where a consumer chooses to do their laundry for example in off-peak periods where prices are lower. Our model of batteries could be used to represent this form of demand shifting.

A different issue arises when the system faces an energy constraint. In the New Zealand case study in Section 4, this corresponds to a dry winter in which hydro reservoir inflows are low. To deal with such an uncertain energy shortage, it is not enough to shift load out of peak periods, electricity must be substituted or foregone. With strongly interconnected systems, substitutes for local electricity can come from imported power. With isolated systems like New Zealand the substitution must come from industrial users of electricity

who reduce production in New Zealand and increase it in other countries where energy supplies are (temporarily) more plentiful.

We model industrial load reduction over a protracted period in each location i using variables $y_{k,i,b,t}(\omega)$, where $k \in \mathcal{I}_i$ indicates a particular type of industrial entity in location i that can shut down to save energy. This incurs an operating loss for the industry of $C_k y_{k,i,b,t}(\omega)$. The maximum amount that load can be reduced at this cost is $U_{k,i}$. The model is flexible enough to provide more of this option (possibly) with fixed costs $K_k(x_{k,i}) + L_k(z_{k,i})$, and increasing operating losses with tranches of increasing marginal cost C_k .

This modeling feature is not intended to capture peak shaving (which is accomplished by the battery model). We therefore add constraints to preclude shutdowns cycling over a short period (*e.g.* between peak and off-peak periods within a day). These constraints take the form

$$\begin{aligned} y_{k,i,b,t}(\omega) &= \bar{y}_{k,i,t}(\omega), \quad b \in \mathcal{B}_t, \\ \bar{y}_{k,i,t}(\omega) &\leq z_{k,i}. \end{aligned}$$

This means that in a feasible solution, every load block in a season t will have the same load reduction. If total shutdown of a plant is required then the second constraint could be modeled by variables $\delta \in \{0, 1\}$ with

$$\bar{y}_{k,i,t}(\omega) \leq U_{k,i} \delta.$$

Alternatively we can interpret a fractional value of δ as a shut over a fraction of a season which reduces load in all load blocks uniformly.

The constraints presented here assume that the industrial load can anticipate the uncertain outcome ω . With no anticipation we would obtain

$$\begin{aligned} y_{k,i,b,t}(\omega) &= \bar{y}_{k,i,t}, \quad \omega \in \Omega, \quad b \in \mathcal{B}_t, \\ \bar{y}_{k,i,t}(\omega) &\leq z_{k,i}, \end{aligned}$$

which is arguably too restrictive as it would require plants to plan to shut in advance, and go through with this even if electricity supply turned out to be plentiful. A practical compromise selects uncertain outcomes that can reasonably be anticipated when they start to take effect (*e.g.* a dry winter) and relaxes the nonanticipativity constraints over these dimensions only. Thus if $\Omega = \Omega_1 \times \Omega_2$, where $\omega_1 \in \Omega_1$ denotes a year climate outcome, and $\omega_2 \in \Omega_2$ denotes other random outcomes that cannot be anticipated then we obtain

$$\begin{aligned} y_{k,i,b,t}(\omega_1, \omega_2) &= \bar{y}_{k,i,t}(\omega_1), \quad (\omega_1, \omega_2) \in \Omega, \quad b \in \mathcal{B}_t, \\ \bar{y}_{k,i,t}(\omega_1) &\leq z_{k,i}. \end{aligned}$$

2.8 Stochastic planning model

We now present a succinct formulation of our stochastic social planning model. It helps to recall that $\omega \in \Omega$ indexes scenario, $i \in \mathcal{I}$ indexes location, $k \in \mathcal{K}_i$

indexes technology at location i , $t \in [0, T]$ indexes season, and $b, b' \in \mathcal{B}_t$ index (season dependent) load blocks. (For reference, a full list of parameters and decision variables for this model is provided in Appendix A.) We seek a solution that minimizes expected capital and operating costs.

$$\begin{aligned}
\text{P: } \min \quad & \mathbb{E}(\psi) \\
\text{s.t.} \quad & \psi(\omega) = \sum_i \sum_{k \in \mathcal{K}_i} (K_k x_{k,i} + L_k z_{k,i}) \\
& \quad + \sum_i Z_i(\omega) \\
Z_i(\omega) = & \sum_{t \in [0, T]} \sum_{b \in \mathcal{B}_t} H_b \sum_{k \in \mathcal{K}_i} C_k y_{k,i,b,t}(\omega) \\
& - V \sum_{t \in [0, T]} \sum_{b \in \mathcal{B}_t} H_b (d_{i,b,t}(\omega) - r_{i,b,t}(\omega)), \\
x_{k,i} \leq & X_{k,i}, \\
z_{k,i} \leq & x_{k,i} + U_{k,i}, \\
y_{k,i,b,t}(\omega) \leq & z_{k,i}, \\
y_{k,i,b,t}(\omega) \leq & \mu_{k,i,b,t}(\omega) z_{k,i}, \\
\sum_{b \in \mathcal{B}_t} H_b y_{k,i,b,t}(\omega) \leq & \nu_{k,i,t}(\omega) \sum_{b \in \mathcal{B}_t} H_b z_{k,i} - s_{i,t} + s_{i,t-1}, \\
r_{i,b,t}(\omega) \leq & d_{i,b,t}(\omega), \\
q_{i,b,t}(\omega) = & \sum_{k \in \mathcal{K}_i} y_{k,i,b,t}(\omega) \\
& + \sum_j \left(\left(1 - \frac{\alpha_{j,i}}{2}\right) f_{j,i,b,t}(\omega) - \left(1 + \frac{\alpha_{i,j}}{2}\right) f_{i,j,b,t}(\omega) \right) \\
& - \sum_{k \in \mathcal{K}_i} \sum_{b' \neq b} g_{k,i,b,b',t}(\omega) \\
& + \sum_{k \in \mathcal{K}_i} \eta_k \sum_{b' \neq b} \frac{g_{k,i,b',b,t}(\omega) H_{b'}}{H_b}, \\
d_{i,b,t}(\omega) \leq & q_{i,b,t}(\omega) + r_{i,b,t}(\omega), \\
\sum_{b \in \mathcal{B}_t} H_b \sum_{b' \neq b} g_{k,i,b,b',t}(\omega) \leq & z_{k,i} D_t, \\
\sum_{b' \neq b} g_{k,i,b,b',t}(\omega) \leq & \beta_k z_{k,i}, \\
f \in & \mathcal{F}, \\
s \in & \mathcal{H}.
\end{aligned}$$

The first-stage decisions in this model are the capacity decisions x and z , and the decisions $s_{i,t}$ for each season t that determine how much energy will be transferred by storage at i from season t to season $(t+1) \bmod T$.

As described above, using different choices of the data μ and ν , we can generate a set of models that will add uncertainty in wind and run-of-river hydro generation. The capital plans that result will be different. Further changes in data lead to another class of models that add uncertainty in stored hydro generation, but still seek a solution that minimizes expected capital and operating costs. The capital plans that result will be different again.

3 Constraints on renewables

All of the models of the previous section can be used to study the effect of adding a constraint on non-renewable generation. Four forms of this constraint will be considered. The first three of these non-renewable constraints hold in expectation or in every outcome ω , while the fourth is a chance-constraint formulation.

3.1 Capacity constraint

This is a first stage constraint on total non-renewable (coal, gas and diesel) capacity:

$$\sum_i \sum_{k \in \mathcal{N}_i} z_{k,i} \leq E, \quad (3)$$

where \mathcal{N}_i represents the set of non-renewable generators at location i . It is independent of scenarios ω . **An alternative form of (3) might impose separate constraints on individual non-renewable technologies to discriminate between coal and gas for example. A constraint that is often discussed sets $E = 0$ in (3), to enforce the closure of all non-renewable generation capacity. Our experiments in section 5 are focused on the costs of imposing such a constraint.**

Instead of imposing the constraint (3) explicitly in the optimization problem, we can introduce a Lagrange multiplier σ for the constraint and move this into the objective $\psi(\omega)$:

$$\psi(\omega) = \sum_i \left(\sum_{k \in \mathcal{K}_i} (K_k(x_{k,i}) + L_k(z_{k,i})) + \sum_{k \in \mathcal{N}_i} \sigma z_{k,i} + Z_i(\omega) \right) - \sigma E.$$

The resulting effect of the Lagrangian form of the constraint is to simply replace the $L_k(z_{k,i})$ term by $L_k(z_{k,i}) + \sigma z_{k,i}$ for each $k \in \mathcal{N}_i$. Thus the capacity constraint essentially amounts to an increase in maintenance cost in the non-renewable technologies. Clearly σ and E are intimately related and we can exogenously parameterize the optimization using either σ or E .

3.2 Generation constraint

The second renewable constraint is imposed on second stage decisions and limits expected non-renewable generation:

$$\mathbb{E} \left[\sum_{t \in [0, T]} \sum_{b \in \mathcal{B}_t} H_b \sum_i \sum_{k \in \mathcal{N}_i} y_{k,i,b,t}(\omega) \right] \leq E. \quad (4)$$

A more restrictive *almost sure* constraint is to impose the regulation in each scenario ω :

$$\sum_{t \in [0, T]} \sum_{b \in \mathcal{B}_t} H_b \sum_i \sum_{k \in \mathcal{N}_i} y_{k,i,b,t}(\omega) \leq E, \quad \forall \omega.$$

Introducing Lagrange multipliers for either of these constraints leads to an adjusted cost optimization parameterized by those multipliers. In the almost sure form of the constraint, for example, the modification to Z_i is as follows:

$$\begin{aligned} Z_i(\omega) = & \sum_{t \in [0, T]} \sum_{b \in \mathcal{B}_t} H_b \left(\sum_{k \in \mathcal{K}_i} C_k y_{k,i,b,t}(\omega) + \sum_{k \in \mathcal{N}_i} \sigma(\omega) y_{k,i,b,t}(\omega) \right) \\ & - V \sum_{t \in [0, T]} \sum_{b \in \mathcal{B}_t} H_b (d_{i,b,t}(\omega) - r_{i,b,t}(\omega)) \\ & - \sigma(\omega) E, \end{aligned}$$

amounting essentially to a scenario and season increase in variable operating cost for non-renewables.

3.3 Emission constraint

The third constraint is a limit E on total emissions from all generation that emits CO₂ (including geothermal and CCS generation). Again, this can be expressed in expectation form:

$$\mathbb{E}\left[\sum_{t \in [0, T]} \sum_{b \in \mathcal{B}_t} H_b \sum_i \sum_{k \in \mathcal{N}_i} e_k y_{k,i,b,t}(\omega)\right] \leq E, \quad (5)$$

or in every scenario ω :

$$\sum_{t \in [0, T]} \sum_{b \in \mathcal{B}_t} H_b \sum_i \sum_{k \in \mathcal{N}_i} e_k y_{k,i,b,t}(\omega) \leq E, \quad \forall \omega.$$

Here e_k denotes an emissions factor for output from plant of type k . Although the data H , e and E could vary by location i and/or season t with minor changes to this constraint, we assume in all our experiments that this is not the case.

It seems unnatural to impose an emission constraint in expectation, since one would not want to admit high emissions in any future state of the world. One should bear in mind, however, that the scenarios (ω_1, ω_2) represent potential weather states for a target year far in the future. In our experiments described in Section 5, ω_1 indexes 13 historical inflow years, each of which is assumed to occur with equal probability, and we compute a steady-state operating policy that assumes the target year demand repeats with random outcome ω_1 in each repetition. An expectation will account for the accumulated emissions from applying this steady-state operating policy over several years, which is the statistic that ultimately affects atmospheric CO₂ levels, rather than e.g. the worst emission outcome in any of these years. Of course this estimate of accumulated emissions involves some error that one might want to take account of in the model to be safe, but this would involve a different form of constraint from an almost-sure one.

The constraint E on emissions from electricity generation can be thought of as a regulatory intervention. In practice these emissions will be traded off against emissions in the rest of the economy (or the world if carbon credits are traded internationally). The shadow price σ thus represents a carbon price, which could be imposed on the electricity sector, or emerge from a general equilibrium model with many sectors apart from electricity. It can be implemented via a modification to Z_i similar to that given above:

$$\begin{aligned} Z_i(\omega) = & \sum_{t \in [0, T]} \sum_{b \in \mathcal{B}_t} H_b \left(\sum_{k \in \mathcal{K}_i} C_k y_{k,i,b,t}(\omega) + \sum_{k \in \mathcal{N}_i} \sigma(\omega) e_k y_{k,i,b,t}(\omega) \right) \\ & - V \sum_{t \in [0, T]} \sum_{b \in \mathcal{B}_t} H_b (d_{i,b,t}(\omega) - r_{i,b,t}(\omega)) \\ & - \sigma(\omega) E. \end{aligned}$$

3.4 Chance-constraint on emissions

We denote the tonnes of CO₂ emissions in scenario ω by $J(\omega)$. We can impose a chance constraint on $J(\omega)$ of the form

$$\mathbb{P}(J(\omega) > 0) \leq \beta.$$

Thus if we were to choose $\beta = 0.5$, and ω denotes potential inflow scenarios (possibly sampled from history), then this constraint would restrict annual emissions to zero in at least 50% of these scenarios. We model this as a mixed integer program using a “big-M” constraint by simply adding the following constraints to the stochastic planning model above:

$$\begin{aligned} J(\omega) &= \sum_{t \in [0, T]} \sum_{b \in \mathcal{B}_t} H_b \sum_i \sum_{k \in \mathcal{N}_i} e_k y_{k, i, b, t}(\omega) \\ J(\omega) &\leq M \delta(\omega) \\ \sum_{\omega} \mathbb{P}(\omega) \delta(\omega) &\leq \beta, \\ \delta(\omega) &\in \{0, 1\}. \end{aligned}$$

In our experiments we used $\omega \in \Omega_1$ instead of the full generality of $\omega \in \Omega$. We do not derive a Lagrangian form of this problem since the primal problem now involves binary variables.

As we show in the case study explored in the next section of the paper, each form of emission constraint results in a different outcome, at least when emissions are not removed entirely from electricity generation when one would expect average and almost-sure outcomes to coincide. These differences in outcomes help illuminate what choice of constraint is appropriate.

4 New Zealand Case Study

The New Zealand Labour Party and Green Party of Aotearoa New Zealand Confidence and Supply Agreement of 2017 (as reproduced in [New Zealand ICCC Terms of Reference \(2019\)](#)) states that the “Government will: Request the Climate Commission to plan the transition to 100 % renewable electricity by 2035 (which includes geothermal) in a normal hydrological year”. **The first versions of this agreement omitted the qualifying clause “in a normal hydrological year”, and there was strong advocacy from environmentalists to plan to shut down all non-renewable electricity generation by 2035. In what follows we have interpreted “100 % renewable electricity by 2035 in a normal hydrological year” as a chance constraint (allowing non-zero emissions in a proportion of non-normal years). We compare this formulation of the constraint with others that either limit emissions explicitly or shut down capacity.**

The social planning model P has been implemented using New Zealand data as part of a project seeking to **estimate the costs of meeting these goals**. The data set for the experiment is provided in the online companion to the paper. Selected parameter values are displayed in tables in this section. We also refer the reader to the tables ([B1-B8](#)) in Appendix B to the paper, and to

the online repository at [Data Repository for ‘Renewable electricity capacity planning with uncertainty at multiple scales’ \(2022\)](#). We give a brief summary here of how the parameters of the model were estimated.

The model has three regions ($i = \text{SI, HAY, NI}$) representing the South Island, lower North Island and Upper North Island respectively. These three regions are joined by nominal transmission lines having capacity 1200MW for SI-HAY and 1000 MW for HAY-NI. We model four seasons ($t = 0, 1, 2, 3$) representing the calendar months January-March, April-June, July-September, October-November.

Demand data for the model at the three locations are estimated from half-hourly metered load for every grid exit point in the national transmission system. These data are archived at [Electricity Market Information System \(2019\)](#). The data are adjusted for wind and photovoltaic generation that has not been recorded, and aggregated into regional demand for each half-hour period in 2017. Wind generation data from each region for years 2005-2017 is similarly aggregated. The total metered demand over the three regions is then sorted from maximum to minimum to give a load-duration curve, and the wind generation data in each year is sorted to give the same order of trading periods as the load. This enables us to identify peak periods in which wind generation is absent and estimate the probability of no wind in a peak load block. From the demand and wind data we create 10 load blocks for each season. The number of hours in each load block is shown in [Table B1](#).

For each load block we estimate a level of demand for 2035 by applying a load growth factor to the residential and commercial components that are expected to increase with population and economic growth. (A large aluminium smelter is excluded from these growth estimates.) The level of demand in each block in 2035 is then increased by [projected increases in load from electric vehicles \(5.7 TWh above 2017 levels\) and industrial electrification \(5.5 TWh above 2017 levels\)](#), based on the forecasts in ([New Zealand ICCG, 2019, p. 41](#)). These increases are allocated to regions proportional to population and uniformly to load blocks². The result is a set of tables of projected load (MW) in each block in each region in each season in 2035 with load blocks shown in [Table B2](#).

As discussed in [section 2.3](#) the scenarios in our model are pairs (ω_1, ω_2) , where ω_1 indexes hydrological data from a historical year chosen with equal probability from $\{2005, 2006, \dots, 2017\}$, and $\omega_2 \in \{0, 1\}$ indexes equal events (such as having no wind in peak demand periods). For example, when k represents run-of-river generation, the parameters $\mu_{k,i,b,t}$ are derived from $\hat{\mu}_{i,t}(\omega_1), \omega_1 = 2005, 2006, \dots, 2017$ which are given in [Table B3](#) for $i = \text{SI}$ and $i = \text{NI}$. Similarly, when k represents hydro reservoir generation the parameters $\nu_{k,i,t}(\omega_1), \omega_1 = 2005, 2006, \dots, 2017$ are given in [Table B5](#) for $i = \text{SI}$ and $i = \text{NI}$.

²Although some factor accounting for overnight charging might be applied here we choose to keep this uniform.

On the other hand, when k represents wind generation the parameters $\mu_{k,i,b,t}(\omega_2)$ are given in Table B7 for $\omega_2 = 1$. The values for $\mu_{k,i,b,t}(\omega_2)$ when $\omega_2 = 0$ are identical except for column b1 which contains 0's. The probability of observing $\omega_2 = 0$ in season t is estimated from historical wind data. When k represents photovoltaic solar generation the parameters $\mu_{k,i,b,t}$ are assumed to be deterministic and are given in Table B6.

The existing capacities of generation technologies in each region were sourced from the Electricity Authority generation database available at [Electricity Market Information System \(2019\)](#). For 2035 we assumed that the coal/gas fired Rankine units at Huntly would be decommissioned as would the Stratford combined cycle plant. This gives a mix of existing capacities as shown in Table 1. Each run of the model proposes limits on new capacity to build of each technology. In our example runs we have chosen possible capacity additions as also shown in Table 1.

Table 1: Capacity of existing plant (MW) that will be available in 2035 and potential electricity capacity increases (MW) by technology and region.

Existing Cap.	SI	HAY	NI
CCGT	0.0	0.0	403.0
CCS	0.0	0.0	0.0
DIESEL	0.0	0.0	155.0
DR	50.0	0.0	0.0
GEOT	0.0	0.0	892.7
HYDROr	840.0	0.0	687.0
HYDROs	2573.0	0.0	1051.0
OCGT	0.0	0.0	350.8
SLOWBATT	0.0	0.0	0.0
MEDBATT	0.0	0.0	0.0
FASTBATT	0.0	0.0	0.0
SOLAR	0.0	0.0	0.0
WIND	0.0	143.0	232.2
Pot. Increase	SI	HAY	NI
CCGT	0.0	0.0	2000.0
CCS	0.0	0.0	2000.0
DIESEL	0.0	0.0	0.0
DR	0.0	0.0	0.0
GEOT	0.0	0.0	542.0
HYDROr	130.5	0.0	0.0
HYDROs	0.0	0.0	0.0
OCGT	0.0	0.0	920.0
SLOWBATT	500.0	500.0	500.0
MEDBATT	500.0	500.0	500.0
FASTBATT	500.0	500.0	500.0
SOLAR	1000.0	1000.0	1000.0
WIND	5000.0	5000.0	5000.0

New capacity incurs an annualized fixed capital cost, and new and existing capacity incurs an annual operations and maintenance cost. The annualized capital cost is a capital recovery factor per MW of capacity that gives the before tax annual revenue that would be required to give an internal rate of return of 8 % (after depreciation and tax) on the capital. Estimates of capital costs for thermal plant have been obtained from [US Energy Information Administration \(EIA\) \(2019\)](#), and costs for CCGT with Carbon Capture and Storage (CCS) were sourced from [Rubin and Zhai \(2012\)](#).

The values of K_k , C_k , and L_k assumed in our models are shown in Table 2. All costs are measured in 2018 New Zealand dollars.

Table 2: Capital costs, variable costs and maintenance costs

Costs	K_k (NZD/MW/Yr)	C_k (NZD/MWh)	L_k (NZD/MW/Yr)
CCGT	138000	70	45000
CCS	242717	75	45000
DIESEL	110400	232	15000
DR	0	1000	0
GEOT	430000	1	150000
HYDRO _r	430000	6	0
HYDRO _s	516000	6	0
OCGT	110400	93	15000
SLOWBATT	48364	0	5000
MEDBATT	163879	0	6000
FASTBATT	314788	0	7000
SOLAR	110400	2	35000
WIND	178000	12	20000

5 Computational results

This section of the paper describes the results of some computational experiments with the social planning model under a number of assumptions. Experiment 1 studies the effect of thermal capacity reduction on average CO₂ emissions. Experiment 2 uses “business-as usual” forecasts of 2035 electricity demand and studies the effect on total investment and expected operating cost of tightening the constraints either on non-renewable generation or on average CO₂ emissions. Experiment 3 assumes more electricity demand in 2035 (due to electric vehicle growth and industrial electrification) and studies the effect on expected system cost of tightening constraints either on non-renewable generation or on average CO₂ emissions. Experiment 4 compares different probabilistic versions of the constraint on CO₂ emissions.

5.1 Experiment 1: Emission Reduction Paradox

The first experiment we carried out tested a [counterintuitive](#) conjecture that decreasing the capacity of thermal plant could increase CO₂ emissions. This

effect was first noticed in a more detailed model developed by [Fulton \(2018\)](#), solved using a version of the SDDP algorithm. In our model we removed the CO₂ reduction constraints and amended [Table 1](#) so that each region had 1200MW of CCGT, no OCGT or DIESEL, and no changes in generation capacity were allowed. The value of \hat{s} was set to 0 for simplicity. This mix of generation gave annual average CO₂ emissions of 4409 kt. We then reduced the CCGT capacity to 700MW in each region, while all other capacities remained unchanged. The model then gave annual average CO₂ emissions of 4428 kt.

The average energy generated by geothermal plant is the same in each run, so the difference in average emissions results from CCGT generation. The average energy generated by CCGT plant in each season in these two cases is shown in [Table 3](#). One can see that the CCGT generation in the 700MW case

Table 3: Average CCGT generation in season t

GWh	0	1	2	3	Total
1200 MW	2353	2693	2388	2419	9853
700 MW	2673	2836	2018	2376	9903

is higher overall, and is higher on average in the first half of the year.

The optimal values of the first-stage storage levels $\bar{s}_{i,t}$ are not unique. It is easy to see that one can add or subtract a constant from all of them and remain feasible as long as the values remain between their bounds. To make a comparison, we have normalized the results so that both runs have the same storage at the end of period 2. The resulting figures are shown in [Table 4a](#) (for 1200 MW) and [Table 4b](#) (for 700 MW).

Table 4: Reservoir storage at the end of season t

(a) CCGT capacity 1200MW					(b) CCGT capacity 700MW				
GWh	0	1	2	3	GWh	0	1	2	3
SI	1809	1526	0	943	SI	1736	1526	0	957
NI	291	20	374	761	NI	590	390	374	691
Total	2136	1526	374	1683	Total	2326	1916	374	1648

Observe that with lower thermal capacity ([Table 4b](#)) the reservoir levels at the end of period 3 are about the same but the model gives a higher average reservoir volume 2326 GWh at the end of period 0 than in the higher thermal capacity case ([Table 4a](#) with 2136 GWh). This increase in reservoir levels requires additional thermal generation to attain the higher storage level, which is put in place as a hedge against the chance of a dry winter. The additional storage hedge is not needed when 1200MW of CCGT capacity is available to be used in [period 1](#) case of low inflows.

Clearly this conclusion requires the use of the stochastic model to provide value for hedging, and using the water levels as a first stage variable enables the planning model to capture the observed effect. More generation (**from less thermal capacity**) leads to higher emissions. This effect, which can be observed over a wide range of data values, is examined in more detail in [Fulton \(2018\)](#).

In most electricity systems, closing down the heaviest emitting plant will decrease emissions, and so the closure of coal plants receives strong support in climate policy. In a hydro-dominated electricity system with uncertain inflows and high costs of shortage (like New Zealand’s), more care must be taken in assessing such policy decisions.

5.2 Experiment 2: Capacity versus Generation

In the second experiment, we investigated the effect of varying the level of the renewable constraints on the model. The alternative formulations of these constraints ((3), (4), and (5)) impose bounds E on non-renewable capacity, non-renewable energy and average CO₂ emissions respectively. The constraints are made progressively more restrictive by a parameter θ that increases from 0 to 1. The right-hand side E of each constraint ((3), (4), and (5)) is replaced by $(1-\theta)\bar{E}$, where \bar{E} denotes the 2017 level of the appropriate quantity (including predetermined closures in the case of (3)).

It is important to be clear what θ measures, especially when the constraint (5) is imposed. In this case the right-hand side E of constraint (5) is replaced by $(1-\theta)\bar{E}$, where \bar{E} equals the 2017 level of emissions from electricity generation (three million tonnes). Here a value of $\theta = 0.5$ does not mean a 50 % renewable electricity system, but a system that emits on average 50 % of the electricity CO₂ emissions of 2017 (which comes from about 15 % of generated electricity in 2017). So, in terms of average emission levels, a given value of θ amounts to an $(85 + 15\theta)$ -%-renewable electricity system.

In Figures 1a and 1b, θ is shown on the horizontal axis, and capacity constraint (3) from Section 3.1 is depicted by the “NR capacity redn” bars, the generation constraint (4) from Section 3.2 is depicted by the “NR energy redn” bars, and the emission constraint (5) from Section 3.3 is depicted by the “CO2 redn” bars. The y-axis for Figure 1a is kt of carbon and in Figure 1b it depicts the annual cost in (2018)\$B NZ. Since (renewable) geothermal and CCS emit some CO₂ (so renewable is not the same as no carbon emission), Figure 1a shows that a value of $\theta = 1$ yields modest reductions in actual CO₂ emissions if we impose only the capacity or energy reduction constraints (3) or (4). When θ represents percentage reductions in actual CO₂ emissions (including those from geothermal and CCS) the green bars in Figure 1b show that the cost increases are fairly modest (27%) up to $\theta = 0.95$, but are around 45 % for zero carbon emissions ($\theta = 1$).

In summary, Experiment 2 shows that outcomes from reducing “non-renewable” capacity (blue bars) is different from and more expensive than reducing “non-renewable” energy (orange bars) unless these are both set to

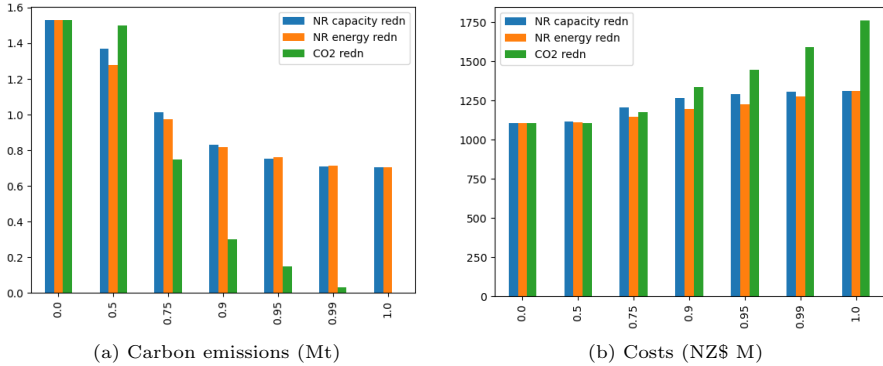


Fig. 1: Increasing θ on constraints

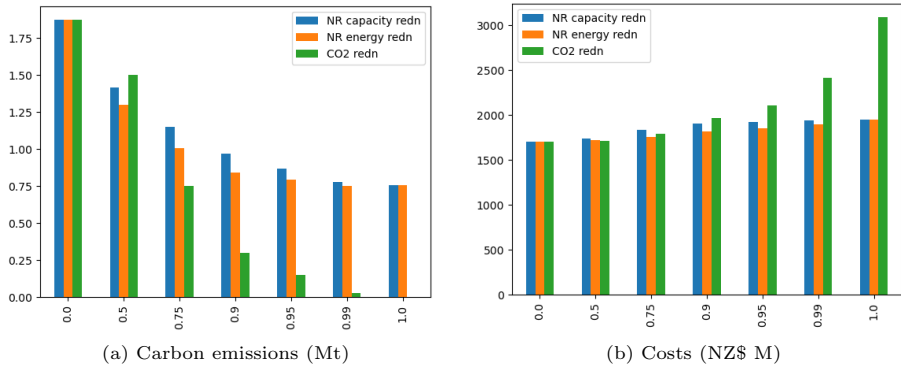


Fig. 2: Increasing θ on constraints (increased load)

zero (when $\theta = 1$). Focusing investment on emission reduction (green) eventually gives zero emissions (when $\theta = 1$) but costs significantly more as geothermal generation and CCS are precluded from the mix at this point.

5.3 Experiment 3: Increased Electricity Demand

The next experiment we carried out compared the expected cost of meeting targets on nonrenewable capacity as compared with meeting targets on non-renewable energy, but with increased forecast electricity load (see Table B8 in Appendix B) arising from electric vehicles and conversion of industrial process heat from gas and coal to electricity. [The increased demand for electricity amplifies the effects seen in Experiment 2.](#)

The bars denoted “CO₂ redn” in Figure 2 show that the cost of actually reaching zero CO₂ emissions (without geothermal or CCS) increases substantially as we approach the limit. For completeness, in the emission constraint

case shown in Figure 3, we split the costs out into four bars depicting the investment cost, the cost of maintenance, the expected operating cost, and the expected cost of lost load.

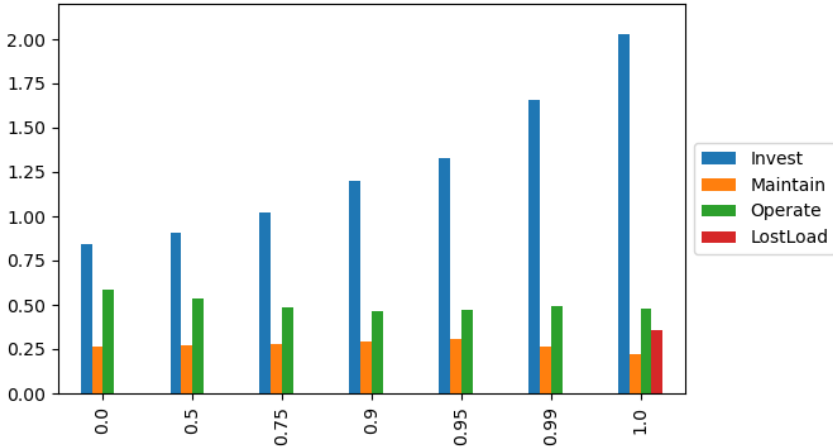


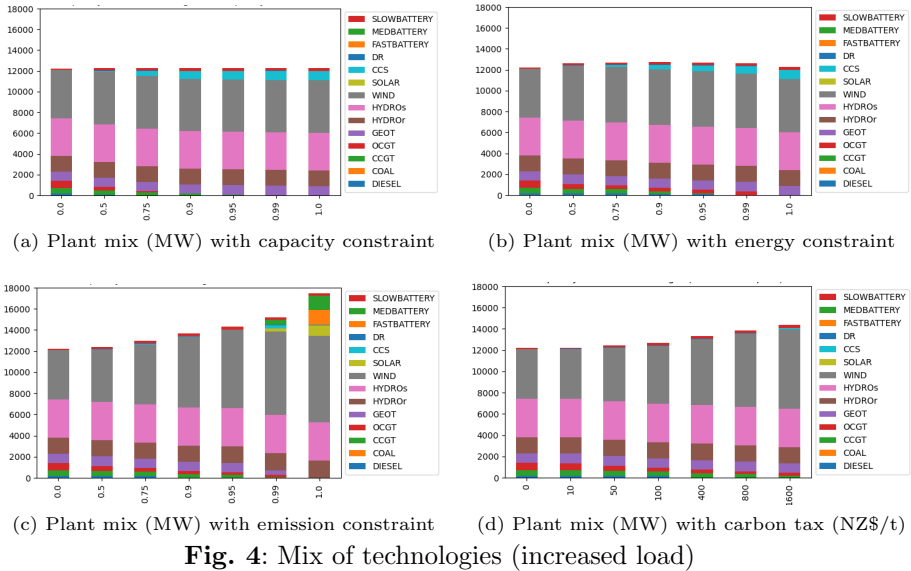
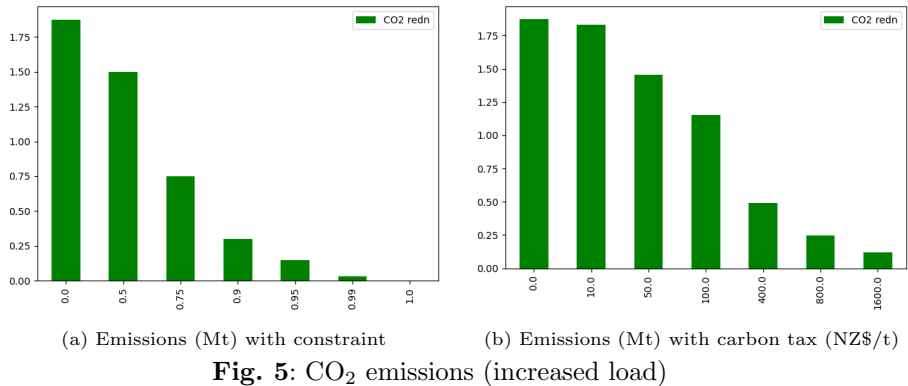
Fig. 3: Increasing θ on constraints (increased load)

The mix of technologies used in the solutions (for the increased load case) is shown in Figure 4. The capacity and energy reduction mixes shown in Figure 4a and Figure 4b are almost indistinguishable, although Figure 4b does retain more non-renewable capacity (CCGT and OCGT) at around 75-90% reduction in non-renewable energy. At this level of energy reduction some non-renewable plants are kept open (violating the non-renewable capacity constraint) but used only sparingly to provide hydro firming in dry years, so meeting the non-renewable energy constraint.

The mix for emission reduction is more diverse as the level of emissions becomes small. Geothermal is removed (since it is a CO₂ emitter) and replaced by large amounts of wind coupled with some solar and battery capacity. We have modeled three different forms of battery named SLOWBATTERY, MED-BATTERY and FASTBATTERY with β_k equal to 0.1617, 0.8846, 2.7660 MW/MWh respectively, and values of K_k and L_k as shown in Table 2. It is interesting to note that CCS comes into the mix when $\theta = 0.99$, but cannot be present at the 100 % level.

As mentioned earlier in the paper, we are able to replace the parametric constraint on emissions by a carbon tax. The figures 4c and 4d could be made identical by suitable choices for the carbon tax, but we give a representative set of values only in Figure 4d. Note that a value of the carbon tax of around \$400 per tonne leads to similar capacity mix (Figure 4d) as the $\theta = 0.90$ system (Figure 4c).

The CO₂ emissions from these two solutions are shown in Figure 5. The choice of \$400 tax gives CO₂ emissions (see Figure 5b) of about 500,000 t,

**Fig. 4:** Mix of technologies (increased load)**Fig. 5:** CO₂ emissions (increased load)

from CCGT, OCGT and geothermal plant. The choice of $\theta = 0.90$ gives CO₂ emissions (see Figure 5a) of about 250,000 t, from CCGT, OCGT and geothermal plant. The \$400 tax is not sufficient to make these non-renewable plant reduce output enough to get down to 250,000 t of CO₂ emissions. As shown by the penultimate bar in Figure 5b, a tax closer to \$800 is needed to make these reductions.

5.4 Experiment 4: Forms of Emission Constraint

In this experiment, we investigate the effect of using different probabilistic versions of the [constraints on non-renewable capacity and generation](#) as described in [Section 3](#).

5.4.1 Almost sure constraint

Figure 6 shows the results for meeting the [constraints in the almost-sure sense](#). We compare these with the corresponding graphs for expectation constraints shown in [Figure 2](#). Since capacity expansion is a first-stage decision, the “NR capacity redn” outcomes are the same as those shown in [Figure 2](#) for constraining expected emissions. Significant differences between [Figure 2](#) and [Figure 6](#) for the “NR energy redn” and “CO₂ redn” outcomes are observed only at relatively low levels of CO₂ reduction. The “NR energy redn” bar reduces height significantly for the 0.0 average reduction case. In [Figure 2](#) this bar measures average non-renewable energy production when this is constrained to be below 2017 levels, whereas the orange bar in [Figure 6](#) measures average non-renewable energy generation when this generation is constrained to be below 2017 levels *in every scenario*. The latter is more restrictive and will give a lower average. In fact, there is a single year, 2005, in which the emissions are significantly higher than all the others in the average case, but is compensated for by reduced emissions in other years. Similar (albeit less dramatic) differences are seen for the 0.5 average reduction case, and then these differences disappear as the emissions constraints become stricter, and non-renewable energy reductions in every scenario become necessary. When the average reduction factor is 1.0, the constraints are identical and the outcomes shown in [Figure 2](#) and [Figure 6](#) are the same.

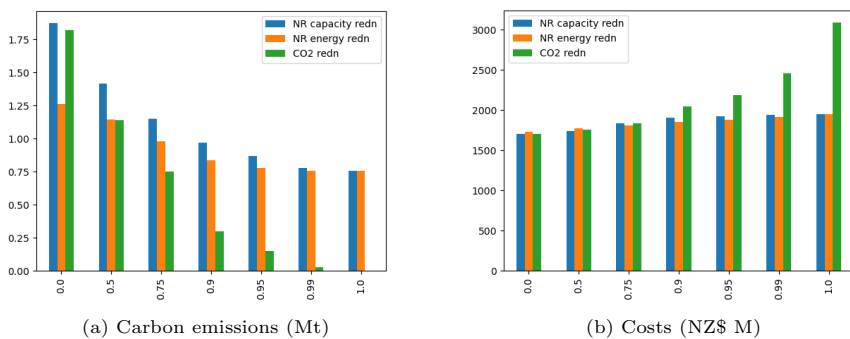


Fig. 6: Increasing θ on constraints, almost sure case (increased load)

5.4.2 Chance constraint

The next results compute the cost of meeting a chance constraint (with original and increased load data). The chance constraint requires that the system has zero CO₂ emissions in 7 out of the 13 scenarios indexed by {2005, 2006, . . . , 2017}. Our goal here is to study the effects of a constraint that relaxes constraints on emissions in years with abnormal inflows.

The optimal capacity mix for the original load data is shown in Figure 7a and the optimal capacity mix for the increased load data is shown in Figure 7b. The mix of capacities in Figure 7b is commensurate with the mix shown in Figure 4c which is optimal for a renewable level of 100 %.

Figure 8a and Figure 8b show the realized reductions in CO₂ in each scenario in the two load cases. As one would expect, the scenarios in which the zero CO₂ requirement can be violated include the years 2005, 2008 and 2012, all of which had “dry winters” with low reservoir inflows.

Comparing Figure 8a and Figure 8b it is surprising that the CO₂ emissions from the optimal capacity mix decrease as the load increases. This occurs because the increased load case requires increased investment in renewable generation (wind, solar and batteries: see Figure 7a and Figure 7b) in order to have zero emissions in the seven scenarios (2006, 2009, 2010, 2011, 2015, 2016, 2017) as shown in Figure 8b. Once built, renewable technologies have zero short-run marginal cost, so they are cheaper than thermal plant and so are dispatched ahead of thermal plant. This leads to a reduction in CO₂ emissions *in every scenario* even if emissions are constrained in only 7 of these.

Figure 8a and Figure 8b show the realized reductions in CO₂ in each scenario from the chance-constrained capacity choices shown in Figure 7a and Figure 7b. As expected, there are nonzero CO₂ emissions in 6 out of the 13 scenarios, and although the system is 100 % renewable in the other 7 scenarios, the average level of CO₂ emissions in the original load case is about 0.1 Mt, while in the increased load case it is about 0.028 Mt, respectively a 97 % or 99 % reduction in CO₂ emissions from 3 million tonnes in 2017. The expected cost of the chance-constrained solution with the original load is \$1.64 B NZ, while the cost for the chance-constrained solution with increased load is \$ 2.75 B NZ. One can compare these with estimates of costs for “CO₂ redn” in Figure 1b and Figure 2b which are \$1.5 B NZ and \$2.0 B NZ respectively. As one might expect, the cost of average emission reductions that result from solving a model with a literal interpretation of “100% renewable in a normal hydrological year” can be more than the optimal cost from a model that has an explicit constraint on average emissions.

5.5 Experiment 5

In the final experiment we examine a mooted proposal to create a pumped storage facility (Lake Onslow) in the South Island of New Zealand to deal with

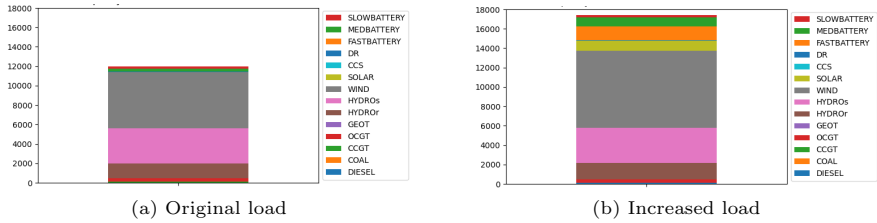


Fig. 7: Capacity mix for model with a chance-constraint on zero emissions in 50% of years

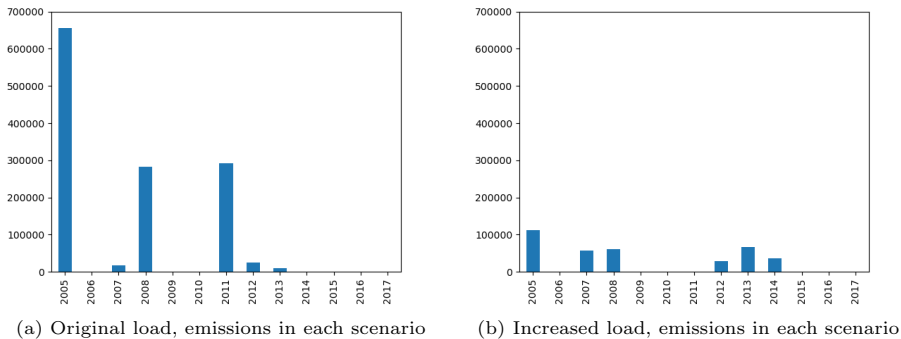


Fig. 8: Emissions for model with a chance-constraint on zero emissions in 50% of years

security of energy supply during “dry winters”.³ Like the rest of the system our model of this proposal is approximate but gives some idea of the expected benefits that such a facility would provide.

To model pumped storage in region i , the stochastic planning model P is altered to include non-negative variables $u_{i,b,t}(\omega)$ and $v_{i,b,t}(\omega)$ that represent flows (MW) of energy added to pumped storage and consumed from pumped storage in region i , season t , load block b and scenario ω . These flows are constrained by the capacities chosen for the installed pumps and generators

$$u_{i,b,t}(\omega) \leq x_i^u,$$

$$v_{i,b,t}(\omega) \leq x_i^v,$$

and by the water available for pumping (which we assume is unlimited).

The demand balance constraint in P becomes

$$d_{i,b,t}(\omega) \leq q_{i,b,t}(\omega) + r_{i,b,t}(\omega) - u_{i,b,t}(\omega) + v_{i,b,t}(\omega).$$

³See <https://www.mbie.govt.nz/building-and-energy/energy-and-natural-resources/low-emissions-economy/nz-battery/>

Thus power supply $q_{i,b,t}(\omega)$ can be greater than demand $d_{i,b,t}(\omega)$ in region i , the excess $u_{i,b,t}(\omega)$ being stored. Similarly power supply $q_{i,b,t}(\omega)$ can be less than demand $d_{i,b,t}(\omega)$ in region i , the shortfall being released $v_{i,b,t}(\omega)$ or shed $r_{i,b,t}(\omega)$.

The total amount of energy put into pumped storage must on average balance that extracted with an efficiency loss $\zeta < 1$, giving

$$\zeta \sum_{\omega} \mathbb{P}(\omega) \sum_t \sum_{b \in \mathcal{B}_t} H_b u_{i,b,t}(\omega) = \sum_{\omega} \mathbb{P}(\omega) \sum_t \sum_{b \in \mathcal{B}_t} H_b v_{i,b,t}(\omega).$$

We can also add a constraint on the size R of the reservoir, by limiting the maximum energy that can be released in any year

$$\sum_t \sum_{b \in \mathcal{B}_t} H_b v_{i,b,t}(\omega) \leq R, \quad \omega \in \Omega.$$

The data used for this experiment are based on preliminary estimates made in a report to the Interim Climate Change Committee [Culy \(2019\)](#), and should be regarded as indicative rather than authoritative. The capital cost of the infrastructure required for the Onslow scheme (*e.g.*, land, tunnels, dams) when annualized was estimated to be \$232.2 M. This estimate excludes the cost of generation plant that is chosen by the model to have capacity between 0 and 1000MW at an annualized cost of \$25800/MW/y. Annualized costs were chosen based on cost recovery rates used for stored hydro assuming a lifetime of 40 years. The round trip efficiency of pumped energy was chosen to be $\zeta = 0.8$, and we assumed unlimited storage capacity R . The model was run with and without the Onslow scheme for a range of constraints on expected CO₂ emissions. We focus on results obtained when the bound on these is 150,000t/y, which is about 5% of 2017 emission levels from electricity generation.

The results are shown in [Tables 5 and 6](#). In the absence of Onslow the optimal capacity plan is to build 2 GW of wind at HAY augmented by a 500 MWh battery in SI. The annual cost of this is \$2.105 B. If the Onslow scheme is built then the optimal capacity plan is to install the maximum of 1000 MW generation in the scheme. This saves the cost of a 500 MWh battery in SI, and reduces the need for wind capacity at HAY, which reduces to 1407.4 MW. The annual capital and operating cost is \$1.898 B. If one adds the annual cost of the Onslow infrastructure (\$232.2 M) then the total annual cost is \$2.13 B, which is approximately the same as the annual cost without Onslow. The difference between the annual cost of a system with and without Onslow depends on the admissible level of CO₂ emissions from electricity generation. If the constraint on total CO₂ emissions is relaxed to be above 150,000t/y then the Onslow scheme becomes uneconomic compared with increased investment in thermal plant. Conversely, a stricter constraint on emissions requires more investment in batteries and wind, making the Onslow scheme less expensive in comparison.

Table 5: New capacity built (MW) by technology and region for emissions constraint of 150,000t/y, assuming no Onslow scheme.

Capacity	SI	HAY	NI
ONSLow	0.0	0.0	0.0
SLOWBATT	500.0	500.0	500.0
WIND	0.0	2049.9	5000.0

Table 6: New capacity built (MW) by technology and region for emissions constraint of 150,000t/y, assuming Onslow scheme.

Capacity	SI	HAY	NI
ONSLow	1000.0	0.0	0.0
SLOWBATT	0.0	500.0	500.0
WIND	0.0	1407.4	5000.0

6 Conclusion

This paper has presented a two-stage stochastic programming model for planning the expansion of electricity generation to achieve specific renewable-energy targets. Different policy prescriptions can be modeled using different formulations of the objective function of this model, each of which is shown to yield different capacity mixes and generation outcomes. This serves to illuminate the advantages and drawbacks of different policy choices.

Versions of our model have been applied to a case study using New Zealand data. This study is not intended to compute recommended policy choices, but rather to serve as an illustration of the power of our models. The models show that there are important differences between policies that mandate nonrenewable capacity limits and those that mandate nonrenewable energy (and CO₂) levels. The latter class of model is more aligned with the underlying objective of reducing greenhouse gas emissions. Similarly chance-constrained versions of our model yield less desirable emission outcomes than those that focus on constraining average emissions.

A common theme that emerges from our experiments is that pursuing a 100% renewable electricity system by 2035 will be very expensive in comparison with a less ambitious objective. Moreover closing down all “non-renewable” generation capacity (in order to achieve the 100% target) will not prevent remaining carbon emissions from “renewable” geothermal generation and CCS. And our work shows that if inflows to hydro reservoirs are uncertain then removing non-renewable capacity does not always result in lower emissions. So although it is arguably a useful political commitment, reducing non-renewable electricity generation *capacity* should not be the objective of an emission reduction program which should focus instead on the amounts of non-renewable *generation*.

We also observe that qualifying the 100% renewable electricity target by adding “in a normal hydrological year” leaves a lot of room for interpretation of “normal”, and so could relax constraints on emissions too much. Our chance-constrained interpretation produced zero CO₂ emissions in over 50% of historical years, but gave worse emissions on average than alternative models that constrained this explicitly.

In 2022, in response to advice from the Interim Climate Change Commission, the New Zealand Government recognized [the high costs of meeting their 2017 policy statement](#) and restated in [MBIE: Terms of Reference for Energy Strategy \(2022\)](#) that the 100% renewable electricity target is an aspiration rather than a policy constraint.

Since the models we are considering have long time horizons over which uncertain effects will become realized gradually, there is considerable value in developing a multistage version of our model. [An example of such a multistage model using scenarios is described in Domínguez et al \(2021\)](#). A natural approach to model uncertainty that evolves over different times scales uses multihorizon scenario trees (see [Kaut et al \(2014\)](#)) in which investment decisions are made at nodes of a coarse scenario tree that models long-term uncertainty (such as load and technology advances) and operational decisions are made at the nodes of this tree, subject to short-term uncertainty (as modeled by the scenarios described in this paper). The approach of most models such as that in [Domínguez et al \(2021\)](#) is to treat short-term uncertainty using “representative days” (see e.g. [Baringo and Conejo \(2013\)](#)), but this is not feasible with a system where short-term uncertainty affects hydroelectric storage. Developing a multistage model for the New Zealand electricity system incorporating this feature is the subject of a forthcoming companion paper [Downward and Philpott \(2023\)](#) that has been presented as [Philpott and Downward \(2021\)](#).

A further policy complication in developing social planning optimization models arises from the fact that, in most industrialized countries, electricity is supplied by large generating companies operating in competitive markets. Since these companies will make the investments in new renewable energy, the plans computed from models such as the one in this paper should be aligned with the profits made by these investments. It is well-known that if markets are competitive and complete and if the investors are risk neutral, then a risk-neutral social plan can be shown to correspond to the competitive equilibrium.

This is not necessarily true if investors are risk averse or behave strategically. Future work [Ferris and Philpott \(2023\)](#) will investigate how to price risks appropriately so that the risk measure of the social planner emerges from those of the investors (see [Ralph and Smeers \(2015\)](#); [Kok et al \(2018\)](#); [Ferris and Philpott \(2022\)](#)).

Declarations

6.1 Funding

This project has been supported in part by the US Department of Energy. The paper was completed while the authors were participating in the Mathematics of Energy Systems thematic programme at the Isaac Newton Institute at the University of Cambridge. The authors wish to acknowledge the support of the INI. The results of the paper are based on the research of the authors and do not represent any official view of the New Zealand Interim Climate Committee or the New Zealand Government. The first author acknowledges the support of the Department of Energy under grant DE-AC02-06CH11357. The second author acknowledges the support of the New Zealand Marsden Fund under contract UOA1520.

Appendix A Stochastic planning model formulation

A.1 Sets

$\omega \in \Omega,$	scenarios
$i \in \mathcal{I},$	locations
$k \in \mathcal{K}_i,$	technologies at location i
$t \in [0, T],$	seasons
$b, b' \in \mathcal{B}_t,$	load blocks in season t

A.2 Parameters

$D_t,$	number of days in season t
$H_b,$	number of hours in load block b
$K_k,$	capital cost (\$/MW) of technology k
$L_k,$	operations and maintenance cost (\$/MW) of technology k
$C_k,$	short-run marginal cost (\$/MWh) of technology k
$V,$	value (\$/MWh) of lost load (VOLL)
$d_{i,b,t}(\omega),$	demand (MW) at location i in load block b in season t in scenario ω
$U_{k,i},$	existing capacity (MW) of technology k at location i
$X_{k,i},$	bound on new capacity (\$/MW) of technology k at location i
$\mu_{k,i,b,t}(\omega),$	load factor of technology k at location i in load block b in season t in scenario ω
$\nu_{k,i,t}(\omega),$	inflow factor for hydro storage k at location i in season t in scenario ω
$\alpha_{i,j},$	loss factor for transmission between location i and location j
$\eta_k,$	round-trip efficiency of battery type k
$\beta_k,$	maximum rate of charge (MW/MWh) of battery type k

A.3 Variables

$\psi(\omega)$,	total system disbenefit (\$) in scenario ω
$x_{k,i}$,	new additional capacity (MW) of technology k at location i
$z_{k,i}$,	resulting capacity (MW) of technology k at location i
$Z_{i,t}(\omega)$,	operating disbenefit (\$) at location i in season t in scenario ω
$y_{k,i,b,t}(\omega)$,	generation (MW) of technology k at location i in load block b in season t in scenario ω
$r_{i,b,t}(\omega)$,	load reduction (MW) at location i in load block b in season t in scenario ω
$s_{i,t}$,	hydro storage targets (MWh) to be met at location i in season t (in every scenario)
$q_{i,b,t}(\omega)$,	power production and net import (MW) at location i in load block b in season t in scenario ω
$f_{i,j,b,t}(\omega)$,	power transmission (MW) from location i to location j in load block b in season t in scenario ω
$g_{k,i,b,b',t}(\omega)$,	power (MW) transferred into battery k from block b to block b' at location i in season t in scenario ω

A.4 Formulation

$$\begin{aligned}
\text{P: } \min \quad & \mathbb{E}(\psi) \\
\text{s.t.} \quad & \psi(\omega) = \sum_i \sum_{k \in \mathcal{K}_i} (K_k x_{k,i} + L_k z_{k,i}) \\
& \quad + \sum_i \sum_{t \in [0, T]} Z_{i,t}(\omega) \\
& Z_{i,t}(\omega) = \sum_{b \in \mathcal{B}_t} H_b \sum_{k \in \mathcal{K}_i} C_k y_{k,i,b,t}(\omega) \\
& \quad - V \sum_{b \in \mathcal{B}_t} H_b (d_{i,b,t}(\omega) - r_{i,b,t}(\omega)), \\
& x_{k,i} \leq X_{k,i}, \\
& z_{k,i} \leq x_{k,i} + U_{k,i}, \\
& y_{k,i,b,t}(\omega) \leq z_{k,i}, \\
& y_{k,i,b,t}(\omega) \leq \mu_{k,i,b,t}(\omega) z_{k,i}, \\
\sum_{b \in \mathcal{B}_t} H_b y_{k,i,b,t}(\omega) & \leq \nu_{k,i,t}(\omega) \sum_{b \in \mathcal{B}_t} H_b z_{k,i} - s_{i,t} + s_{i,t-1}, \\
r_{i,b,t}(\omega) & \leq d_{i,b,t}(\omega), \\
q_{i,b,t}(\omega) & = \sum_{k \in \mathcal{K}_i} y_{k,i,b,t}(\omega) \\
& \quad + \sum_j \left(\left(1 - \frac{\alpha_{j,i}}{2}\right) f_{j,i,b,t}(\omega) - \left(1 + \frac{\alpha_{i,j}}{2}\right) f_{i,j,b,t}(\omega) \right) \\
& \quad - \sum_{k \in \mathcal{K}_i} \sum_{b' \neq b} g_{k,i,b,b',t}(\omega) \\
& \quad + \sum_{k \in \mathcal{K}_i} \eta_k \sum_{b' \neq b} \frac{g_{k,i,b',b,t}(\omega) H_{b'}}{H_b}, \\
\sum_{b \in \mathcal{B}_t} H_b \sum_{b' \neq b} g_{k,i,b,b',t}(\omega) & \leq z_{k,i} D_t, \\
\sum_{b' \neq b} g_{k,i,b,b',t}(\omega) & \leq \beta_k z_{k,i}, \\
f & \in \mathcal{F}, \\
s & \in \mathcal{H}.
\end{aligned}$$

Appendix B Data used in New Zealand model

Excel sheets with a full data set and GAMS models are available for download from Data Repository for ‘Renewable electricity capacity planning with uncertainty at multiple scales’ (2022).

Table B1: Number of hours in each load block b in each season $t = 0, 1, 2, 3$.

	b1	b2	b3	b4	b5	b6	b7	b8	b9	b10
0	10	50	100	200	300	300	300	300	300	300
1	10	50	124	200	300	300	300	300	300	300
2	10	50	148	200	300	300	300	300	300	300
3	10	50	148	200	300	300	300	300	300	300

Table B2: Estimated 2035 demand (MW) in each load block b in each season $t = 0, 1, 2, 3$, in each region i .

SI	b1	b2	b3	b4	b5	b6	b7	b8	b 9	b10
0	2194	2152	2113	2055	1989	1913	1845	1752	1620	1473
1	2302	2263	2219	2146	2042	1942	1833	1710	1587	1447
2	2311	2290	2254	2178	2073	1959	1857	1755	1634	1478
3	2188	2189	2170	2096	1999	1924	1873	1778	1670	1498
HAY	b1	b2	b3	b4	b5	b6	b7	b8	b9	b10
0	583	570	550	541	524	502	469	417	355	328
1	744	722	707	665	613	580	545	474	411	364
2	760	735	720	681	633	597	563	500	429	376
3	630	591	570	552	535	512	473	422	369	343
NI	b1	b2	b3	b4	b5	b6	b7	b8	b9	b10
0	3502	3465	3428	3335	3227	3027	2797	2504	2119	1905
1	4196	4106	3912	3656	3427	3264	3012	2635	2250	1981
2	4310	4160	4011	3810	3583	3380	3172	2805	2350	2079
3	3692	3578	3480	3382	3255	3092	2856	2550	2164	1955

Table B3: Parameters $\hat{\mu}_{i,t}$ for run-of-river generation. Since there is no hydro generation possible in the HAY region these data are not estimated.

SI	0	1	2	3	NI	0	1	2	3
2005	0.611	0.471	0.448	0.397	2005	0.400	0.338	0.380	0.413
2006	0.431	0.487	0.437	0.644	2006	0.360	0.510	0.621	0.384
2007	0.492	0.506	0.492	0.612	2007	0.335	0.230	0.512	0.350
2008	0.486	0.413	0.399	0.572	2008	0.209	0.294	0.685	0.378
2009	0.464	0.594	0.531	0.549	2009	0.275	0.292	0.506	0.464
2010	0.495	0.601	0.536	0.579	2010	0.303	0.335	0.603	0.416
2011	0.618	0.539	0.441	0.553	2011	0.405	0.503	0.511	0.402
2012	0.394	0.439	0.522	0.572	2012	0.436	0.432	0.515	0.385
2013	0.498	0.554	0.656	0.592	2013	0.201	0.260	0.339	0.390
2014	0.555	0.601	0.673	0.630	2014	0.209	0.349	0.396	0.348
2015	0.532	0.632	0.598	0.611	2015	0.168	0.413	0.527	0.348
2016	0.532	0.680	0.592	0.647	2016	0.269	0.330	0.545	0.483
2017	0.562	0.381	0.500	0.513	2017	0.356	0.564	0.682	0.450

Table B4: Run-of-river flexibility parameters $\alpha_{i,t,b}$ as estimated from historical run-of-river hydro generation in each region . The sum of $\alpha_{i,b,t}$ weighted by the hours in each block equals the number of hours in season t . The parameters $\mu_{k,i,b,t}$ for k =run-of-river plant are computed to be $\mu_{k,i,b,t} = \alpha_{i,b,t}\hat{\mu}_{i,t}$.

SI	b1	b2	b3	b4	b5	b6	b7	b8	b9	b10
0	1.305	1.305	1.305	1.000	1.000	1.000	1.000	0.946	0.946	0.946
1	1.383	1.383	1.383	1.000	1.000	1.000	1.000	0.922	0.922	0.922
2	1.415	1.415	1.415	1.000	1.000	1.000	1.000	0.904	0.904	0.904
3	1.263	1.263	1.263	1.000	1.000	1.000	1.000	0.939	0.939	0.939
NI	b1	b2	b3	b4	b5	b6	b7	b8	b9	b10
0	1.546	1.546	1.546	1.000	1.000	1.000	1.000	0.903	0.903	0.903
1	1.680	1.680	1.680	1.000	1.000	1.000	1.000	0.861	0.861	0.861
2	1.488	1.488	1.488	1.000	1.000	1.000	1.000	0.887	0.887	0.887
3	1.447	1.447	1.447	1.000	1.000	1.000	1.000	0.897	0.897	0.897

Table B5: Parameters $\nu_{k,i,t}$ for stored hydro generation. Since there is no hydro generation possible in the HAY region these data are not estimated.

SI	0	1	2	3	NI	0	1	2	3
2005	1.141	0.575	0.593	0.637	2005	0.365	0.321	0.451	0.494
2006	0.851	0.729	0.615	1.144	2006	0.370	0.480	0.578	0.466
2007	0.862	0.622	0.594	0.938	2007	0.342	0.306	0.551	0.427
2008	0.893	0.471	0.652	1.140	2008	0.204	0.376	0.754	0.486
2009	0.839	0.832	0.691	0.920	2009	0.286	0.319	0.535	0.480
2010	0.924	0.808	0.680	1.115	2010	0.271	0.407	0.629	0.419
2011	0.803	0.652	0.492	0.957	2011	0.385	0.472	0.499	0.531
2012	0.723	0.517	0.707	0.975	2012	0.422	0.392	0.607	0.451
2013	0.774	0.685	0.774	1.064	2013	0.224	0.375	0.420	0.461
2014	0.759	0.922	0.588	0.988	2014	0.215	0.391	0.453	0.402
2015	0.789	1.016	0.579	0.980	2015	0.213	0.467	0.579	0.361
2016	1.129	0.894	0.613	0.822	2016	0.316	0.393	0.591	0.475
2017	0.723	0.517	0.707	0.975	2017	0.422	0.392	0.607	0.451

Table B6: Estimated parameters $\mu_{k,i,b,t}$ for photovoltaic solar generation as a proportion of capacity.

SI	b1	b2	b3	b4	b5	b6	b7	b8	b9	b10
0	0.158	0.205	0.338	0.318	0.311	0.214	0.253	0.131	0.015	0.003
1	0.016	0.030	0.038	0.067	0.123	0.121	0.077	0.078	0.006	0.001
2	0.008	0.028	0.050	0.084	0.121	0.149	0.162	0.064	0.006	0.001
3	0.409	0.370	0.371	0.375	0.248	0.218	0.230	0.157	0.045	0.017
HAY	b1	b2	b3	b4	b5	b6	b7	b8	b9	b10
0	0.158	0.205	0.338	0.318	0.311	0.214	0.253	0.131	0.015	0.003
1	0.016	0.030	0.038	0.067	0.123	0.121	0.077	0.078	0.006	0.001
2	0.008	0.028	0.050	0.084	0.121	0.149	0.162	0.064	0.006	0.001
3	0.409	0.370	0.371	0.375	0.248	0.218	0.230	0.157	0.045	0.017
NI	b1	b2	b3	b4	b5	b6	b7	b8	b9	b10
0	0.246	0.271	0.348	0.321	0.277	0.185	0.240	0.129	0.013	0.002
1	0.025	0.039	0.050	0.083	0.133	0.143	0.099	0.079	0.008	0.001
2	0.011	0.042	0.081	0.103	0.137	0.152	0.171	0.077	0.010	0.001
3	0.374	0.342	0.340	0.309	0.224	0.202	0.234	0.155	0.036	0.012

Table B7: Estimated parameters $\mu_{k,i,b,t}$ for wind generation for the scenario when wind blows in block 1. The same table applies when wind does not blow in block 1, except that the column headed b1 is replaced by zeroes.

SI	b1	b2	b3	b4	b5	b6	b7	b8	b9	b10
0	0.25	0.18	0.14	0.28	0.37	0.37	0.41	0.37	0.34	0.38
1	0.34	0.18	0.14	0.28	0.37	0.37	0.41	0.37	0.34	0.38
2	0.35	0.17	0.25	0.26	0.27	0.30	0.37	0.36	0.32	0.35
3	0.22	0.11	0.16	0.24	0.29	0.32	0.37	0.33	0.28	0.37
HAY	b1	b2	b3	b4	b5	b6	b7	b8	b9	b10
0	0.35	0.15	0.17	0.36	0.51	0.48	0.46	0.47	0.35	0.54
1	0.30	0.15	0.17	0.36	0.51	0.48	0.46	0.47	0.35	0.54
2	0.44	0.31	0.38	0.42	0.44	0.45	0.53	0.47	0.41	0.61
3	0.32	0.11	0.19	0.35	0.40	0.43	0.48	0.50	0.35	0.48
NI	b1	b2	b3	b4	b5	b6	b7	b8	b9	b10
0	0.28	0.25	0.30	0.40	0.49	0.46	0.48	0.52	0.40	0.55
1	0.52	0.25	0.30	0.40	0.49	0.46	0.48	0.52	0.40	0.55
2	0.36	0.31	0.34	0.35	0.34	0.37	0.45	0.41	0.33	0.45
3	0.19	0.13	0.23	0.28	0.38	0.45	0.41	0.42	0.31	0.48

Table B8: Increased estimated 2035 demand (MW) from PEVs and electrification in each load block b in each season $t = 0, 1, 2, 3$, in each region i .

SI	b1	b2	b3	b4	b5	b6	b7	b8	b9	b10
0	2550	2506	2442	2346	2255	2159	2076	1932	1789	1630
1	2579	2538	2497	2410	2285	2169	2024	1871	1736	1585
2	2588	2565	2532	2442	2316	2186	2048	1916	1784	1615
3	2544	2543	2499	2388	2265	2171	2104	1959	1839	1655
HAY	b1	b2	b3	b4	b5	b6	b7	b8	b9	b10
0	787	771	742	713	681	649	610	528	463	429
1	913	887	876	825	760	718	668	577	510	456
2	929	900	890	841	780	736	686	602	528	468
3	834	791	762	724	693	659	614	533	476	444
NI	b1	b2	b3	b4	b5	b6	b7	b8	b9	b10
0	4355	4315	4223	4046	3876	3641	3376	2967	2551	2315
1	4891	4798	4604	4312	4029	3839	3513	3059	2644	2352
2	5005	4852	4703	4466	4185	3955	3673	3229	2743	2450
3	4544	4428	4274	4093	3904	3707	3435	3013	2597	2365

References

- Baringo L, Conejo A (2013) Correlated wind-power production and electric load scenarios for investment decisions. *Applied energy* 101:475–482
- Bishop P, Bull B (2008) The future of electricity generation in New Zealand. In: 13th annual conference of the New Zealand Agricultural and Resource Economics Society, Nelson, New Zealand, pp 28–29
- Boffino L, Conejo A, Sioshansi R, et al (2019) A two-stage stochastic optimization planning framework to decarbonize deeply electric power systems. *Energy Economics* 84:104,457
- Cheng B, Powell W (2016) Co-optimizing battery storage for the frequency regulation and energy arbitrage using multi-scale dynamic programming. *IEEE Transactions on Smart Grid* 9(3):1997–2005
- Culy J (2019) Report to the Interim Climate Change Committee. Tech. rep., downloadable from <https://www.iccc.mfe.govt.nz>
- Data Repository for ‘Renewable electricity capacity planning with uncertainty at multiple scales’ (2022) <https://www.cs.wisc.edu/~ferris/data/100percent>
- De Jonghe C, Hobbs B, Belmans R (2012) Optimal generation mix with short-term demand response and wind penetration. *IEEE Transactions on Power Systems* 27(2):830–839
- Domínguez R, Vitali S, Carrión M, et al (2021) Analysing decarbonizing strategies in the european power system applying stochastic dominance constraints. *Energy Economics* 101:105,438
- Downward A, Philpott A (2023) Multistage models for 100 percent renewable electricity. Tech. rep., Electric Power Optimization Centre (EPOC), Auckland, NZ
- Egging R, Fleten SE, Grønvik I, et al (2016) Linear decision rules for hydropower scheduling under uncertainty. *IEEE Transactions on Power Systems* 32(1):103–113
- Electricity Market Information System (2019) Tech. Rep. Downloaded from <https://www.emi.ea.govt.nz>, New Zealand Electricity Authority
- Ferris M, Philpott A (2022) Dynamic risked equilibrium. *Operations Research* 70(3):1933–1952
- Ferris M, Philpott A (2023) Equilibrium models for 100 percent renewable electricity. Tech. rep., in preparation.

- Fishbone L, Abilock H (1981) MARKAL , a linear-programming model for energy systems analysis: Technical description of the bnl version. *International Journal of Energy Research* 5(4):353–375
- Fulton B (2018) Security of supply in the New Zealand electricity market. BE Honours Project Report, Department of Engineering Science, University of Auckland, <https://www.epoc.org.nz/theses/FultonReport.pdf>
- Graf C, Marcantonini C (2017) Renewable energy and its impact on thermal generation. *Energy Economics* 66:421–430
- Graf C, Wozabal D (2013) Measuring competitiveness of the EPEX spot market for electricity. *Energy Policy* 62:948–958
- Joskow P (2006) Competitive electricity markets and investment in new generating capacity. Tech. rep., AEI-Brookings Joint Center Working Paper 06-14
- Kaut M, Midthun K, Werner A, et al (2014) Multi-horizon stochastic programming. *Computational Management Science* 11(1-2):179–193
- Khazaei J, Powell W (2017) SMART-Invest: a stochastic, dynamic planning for optimizing investments in wind, solar, and storage in the presence of fossil fuels. the case of the PJM electricity market. *Energy Systems* pp 1–27
- Kok C, Philpott A, Zakeri G (2018) Value of transmission capacity in electricity markets with risk averse agents. Tech. Rep. www.epoc.org.nz/papers/TransmissionPaperOperationsResearch.pdf, EPOC Working Paper
- Loulou R (2008) ETSAP-TIAM: the TIMES integrated assessment model. Part II: Mathematical formulation. *Computational Management Science* 5(1-2):41–66
- Loulou R, Labriet M (2008) ETSAP-TIAM: the TIMES integrated assessment model Part I: Model structure. *Computational Management Science* 5(1-2):7–40
- Mason I, Page S, Williamson A (2010) A 100% renewable electricity generation system for New Zealand utilising hydro, wind, geothermal and biomass resources. *Energy Policy* 38(8):3973–3984
- Mason I, Page S, Williamson A (2013) Security of supply, energy spillage control and peaking options within a 100% renewable electricity system for New Zealand. *Energy Policy* 60:324–333

- Masse P, Gibrat R (1957) Application of linear programming to investments in the electric power industry. *Management Science* 3(2):149–166
- MBIE: Terms of Reference for Energy Strategy (2022) <https://www.mbie.govt.nz/dmsdocument/25373-terms-of-reference-new-zealand-energy-strategy>
- Merrick JH (2016) On representation of temporal variability in electricity capacity planning models. *Energy Economics* 59:261–274
- New Zealand ICCC (2019) Accelerated Electrification. Tech. Rep. Downloaded from <https://www.climatecommission.govt.nz/public/Advice-to-govt-docs/ICCC-accelerated-electrification-report.pdf>, New Zealand Interim Climate Change Committee
- New Zealand ICCC Terms of Reference (2019) Tech. Rep. Downloaded from <https://www.iccc.mfe.govt.nz/who-we-are/terms-of-reference>, New Zealand Interim Climate Change Committee
- Philpott A, Downward A (2021) Renewable energy capacity planning using JuDGE. URL <https://www.epoc.org.nz/ww2021.html>
- Pineda S, Morales J (2018) Chronological time-period clustering for optimal capacity expansion planning with storage. *IEEE Transactions on Power Systems* 33(6):7162–7170
- Ralph D, Smeers Y (2015) Risk trading and endogenous probabilities in investment equilibria. *SIAM Journal on Optimization* 25(4):2589–2611
- Rubin E, Zhai H (2012) The cost of carbon capture and storage for natural gas combined cycle power plants. *Environmental Science & Technology* 46(6):3076–3084
- Short W, Sullivan P, Mai T, et al (2011) Regional Energy Deployment System (ReEDS). Tech. rep., National Renewable Energy Lab.(NREL), Golden, CO (United States)
- Sioshansi R, Denholm P, Jenkin T, et al (2009) Estimating the value of electricity storage in PJM: Arbitrage and some welfare effects. *Energy Economics* 31(2):269–277
- Skar C, Doorman G, Tomasgard A (2014) The future European power system under a climate policy regime. In: 2014 IEEE International Energy Conference (ENERGYCON), IEEE, pp 318–325
- Stoft S (2002) *Power System Economics*. IEEE Press, Piscataway

US Energy Information Administration (EIA) (2019) Capital cost estimates for utility-scale electricity generation. Downloaded from <https://www.eia.gov>

Wu A, Philpott A, Zakeri G (2017) Investment and generation optimization in electricity systems with intermittent supply. *Energy Systems* 8(1):127–147

Xi X, Sioshansi R, Marano V (2014) A stochastic dynamic programming model for co-optimization of distributed energy storage. *Energy Systems* 5(3):475–505